



**MODELING AND ANALYSIS OF HIGH
ENERGY LASER WEAPON SYSTEM
PERFORMANCE IN VARYING
ATMOSPHERIC CONDITIONS**

THESIS

Megan P. Melin, DR-II Civilian, USAF

AFIT-OR-MS-ENS-11-27

**DEPARTMENT OF THE AIR FORCE
AIR UNIVERSITY**

AIR FORCE INSTITUTE OF TECHNOLOGY

Wright-Patterson Air Force Base, Ohio

APPROVED FOR PUBLIC RELEASE; DISTRIBUTION UNLIMITED.

The views expressed in this thesis are those of the author and do not reflect the official policy or position of the United States Air Force, Department of Defense, or the United States Government.

AFIT-OR-MS-ENS-11-27

MODELING AND ANALYSIS OF HIGH ENERGY LASER WEAPON SYSTEM
PERFORMANCE IN VARYING ATMOSPHERIC CONDITIONS

THESIS

Presented to the Faculty

Department of Operational Sciences

Graduate School of Engineering and Management

Air Force Institute of Technology

Air University

Air Education and Training Command

In Partial Fulfillment of the Requirements for the
Degree of Master of Science in Operations Research

Megan P. Melin, B.S.

DR-II Civilian, USAF

September 2011

APPROVED FOR PUBLIC RELEASE; DISTRIBUTION UNLIMITED.

MODELING AND ANALYSIS HIGH ENERGY LASER WEAPON SYSTEM
PERFORMANCE IN VARYING ATMOSPHERIC CONDITIONS

Megan P. Melin, B.S.
DR-II Civilian, USAF

Approved:

// SIGNED//

9/12/2011

Dr. J. O. Miller (Chairman)

date

// SIGNED//

9/12/2011

Dr. Raymond Hill (Member)

date

Abstract

This thesis addresses two primary concerns relating to Directed Energy (DE) models and tests: need for more use of Design of Experiment (DOE) in structuring DE models and tests, and lack of modeling atmospheric variability in High Energy Laser (HEL) weapon system propagation models and tests. To address these concerns we use a DOE factorial design to capture main, interaction, and non-linear effects between modeled weapon design and environmental factors in a well defined simulated Air-to-Ground HEL engagement scenario. The scenario modeled considers a B1-B aircraft in the 2022 timeframe equipped with an HEL weapon, irradiating a ground target from 30K feet altitude. The High Energy Laser End-to-End Operational Simulation (HELEEOS), developed by the AFIT Center for Directed Energy (CDE), is used to model HEL propagation. Atmospheric variability is incorporated by using input from the Laser Environmental Effects Definition and Reference (LEEDER) model based on randomly selected daily meteorological data (METAR) for a specific geographic location. Results clearly indicate the practical significance of a number of HEL weapon design and environmental factors, to include a number of previously unidentified interactions and non-linear effects, on the final energy delivered to a target for our modeled scenario.

Acknowledgments

I would like to express my sincere appreciation to my faculty advisor, Dr J.O. Miller for his mentoring, direction, and encouragement throughout the course of this thesis research. I appreciate the expertise in modeling and simulation he has brought to the table and all I have learned through his teaching. I would like to extend a million thanks to my civilian advisor, Dr Raymond Hill, who has dedicated hours outside of class helping me to understand the concept of Design of Experiments, the application of Response Surface Methodology, and solely being responsible for enabling me to pursue a masters with AFIT. Both Dr Miller and Dr Hill have been extremely flexible with my requirements to apply operations research to address Directed Energy problem areas.

I would also like to thank members of AFIT's physics department; Rick Bartell, Dr Steve Fiorino, and Dr Sal Cusamano for providing me their subject matter expertise in laser systems, HELEEOS and LEEDR models, and giving me guidance on where to find data, how improvise model modifications, and how to fix the models when I accidentally "broke" them

Megan P. Melin

Table of Contents

Abstract	iv
Acknowledgments	v
List of Figures	ix
List of Tables	xi
I. Introduction	1
1.1 Background & Problem Significance.....	1
1.11 Introduction to High Energy Lasers	2
1.12 High Energy Laser Performance Modeling	3
1.13 Current High Energy Laser Test Practices	4
1.2 Problem Statement	4
1.3 Problem Approach and Scope	5
1.31 Objectives	7
1.32 Assumptions	7
1.4 Thesis Overview	7
II. Background & Literature Review	9
2.1 Theories of the Statistical Atmosphere	9
2.11 Extinction	11
2.12 Turbulence	12
2.13 Atmospheric Models – LEEDR	14
2.14 HEL Scaling Model – HELEEOS	16
2.15 Target Lethality Modeling	17
2.16 JMP Statistical Tool	18
2.2 Design of Experiment.....	18
2.21 Terminology	19
2.22 Seven Stages of Design of Experiment	19
2.3 Response Surface Methodology	22
2.4 Case Studies – Analysis & Results	23
III. Research Methodology	25
3.1 Chapter Overview	25

3.2	Context of the problem.....	25
3.3	Modeling Assumptions	27
3.4	Modeling Process and Inputs	29
3.41	LEEDR Inputs	30
3.42	HELEEOS Inputs	31
3.5	Model Modifications to Simulate Variability of Atmospheric Effects	32
3.51	Absorption & Scattering Data from 14 th Weather Squadron	33
3.52	Turbulence Random Multiplier	33
3.53	Platform Jitter Input as a Random Variable	34
3.6	DOE - Methodology and Experimental Design	35
3.61	Defining the Baseline Mission Scenario and Response	35
3.62	Design Factor, Level, and Range Selection	37
3.63	Experimental Design Selection	38
3.7	Summary	38
IV.	Results and Analysis of Key Design Factors	40
4.1	Experienced-Based Expectations of the Research	40
4.2	Experimental Design	40
4.21	Key Aspects to a Good Model	42
4.22	Full Model Results	43
4.23	Full Model With Poor Visibility Conditions Removed	48
4.24	Side-by-Side Comparison of Models	50
4.25	Response Surface of Full Model	52
4.26	A look at Thermal Blooming	56
4.3	Optimal System Design & Test Design for the Specified Mission Scenario.....	57
4.4	Summary	58
V.	Conclusions and Recommendations.....	60
5.1	Summary of Key Contributions	60
5.2	Key Findings	60
5.3	Caveats on Research.....	63
5.4	Recommendations for Future Work	63

5.5 Implications for Directed Energy Testing	63
Appendix A. $3^{4-1} \times 4^1$ Fractional Experimental Design	65
Appendix B. LEEDR Varied Inputs (Experimental Design & Nuisance Factors)	68
Appendix C. Turbulence and Jitter Variable Inputs into HELEEOS	72
Appendix D. Design Points with Associated Response Variables	76
Appendix E. Blue Dart.....	81
Bibliography	84

List of Figures

Figure 1: Model Process for an Air-to-Ground HEL Engagement Model	6
Figure 2: Diagram Depicting Various Atmospheric Layers and Air Temperature (Andrews and Phillips, 2005).....	10
Figure 3: Example of How Variations in Refractive Index Affect Phase of Light. Note that a lower n implies faster propagation speed (Perram et al., 2010)	13
Figure 4: Example of How Turbulence Effects the Wavefront of Electromagnetic Energy (Perram et al., 2010)	13
Figure 5: LEEDR Geographic Locations.....	15
Figure 6: Relationship of Real Systems to their Empirical Models.....	21
Figure 7: Fishbone Diagram Showing Factor Influences	26
Figure 8: Fishbone Diagram Characterizing Factors	27
Figure 9: Modeling and Analysis Process	30
Figure 10: LEEDR Constant Inputs	31
Figure 11: HELEEOS Constant Inputs	32
Figure 12: Turbulence Multiplier Distribution	34
Figure 13: Platform Jitter Distribution.....	35
Figure 14: Monthly mean SST calculated from the gridded GTSP data from 1990 to 2008 during (top) January and (bottom) July (Fiorino, 2008)	36
Figure 15: Residuals Evaluated for Fit to Normal Distribution.....	45
Figure 16: Residual by Predicted Plot	45
Figure 17: Normal Distribution of Residuals (with Poor Visibility Conditions Removed)	49
Figure 18: Residual by Predicted	50
Figure 19: Residual by Predicted (with Square Root Transform on Response)	50
Figure 20: Response Surface of Slant Range ² vs. PIB.....	53
Figure 21: Response Surface of Wavelegth ² vs. PIB.....	53
Figure 22: Response Surface of Power ² vs. PIB	53
Figure 23: Response Surface of Power*Slant Range vs. PIB.....	54
Figure 24: Response Surface of Power*Aperture vs. PIB	54

Figure 25: Response Surface of Power*Wavelength vs. PIB 55

Figure 26: Response Surface of Slant Range*Beam Quality vs. PIB..... 55

Figure 27: Response Surface of Aperture Size*Beam Quality vs. PIB 56

List of Tables

Table 1: Design Factors - Levels and Range Varied	38
Table 2: Design Factors - Levels and Range Varied	41
Table 3: Parameter Estimates.....	44
Table 4: Analysis of Variance.....	46
Table 5: Parameter Estimates and Contribution to Power in Bucket (PIB).....	47
Table 6: Lack of Fit.....	48
Table 7: Full Model without Poor Visibility - Parameter Estimates	48
Table 8: Model Comparisons - With and Without Poor Visibility Conditions	51
Table 9: Parameter Effects in Relation to Thermal Blooming.....	57
Table 10: Solution to Design	58
Table 11: Model Comparisons - With and Without Poor Visibility Conditions	62

MODELING AND ANALYSIS HIGH ENERGY LASER WEAPON SYSTEM PERFORMANCE IN VARYING ATMOSPHERIC CONDITIONS

I. Introduction

1.1 Background & Problem Significance

The Air Force has been leading the development of high energy laser (HEL) science and technology for aircraft applications since the early 1970's. Three Air Force programs have attempted to integrated HEL weapons into aircraft. The first was the Airborne Laser Laboratory (ALL), integrating a Chemical Oxygen Iodine Laser (COIL) Laser which demonstrated shoot down of AMRAAM missiles. The second was the Airborne Laser (ABL) Program, integrating an HEL onto a Boeing 747 designed to shoot down Theater Ballistic Missiles. The third was the Air Tactical Laser (ATL), integrating an HEL into a C-130 designed to negate moving ground vehicles. Although the performance of these laser weapon systems did not meet Air force expectations, they did advance the technology into higher maturity levels.

Aside from design and engineering hurdles still to overcome with integrating HEL weapons into aircraft, a bigger scientific challenge the US Air Force will face in the very near future is how to improve or simply maintain laser beam propagation through the atmosphere given varying weather conditions. The Government Accounting Office recognizes that atmospheric compensation for the airborne laser is a critical program risk element. (Committees March, 2005).

Atmospheric interferences come in many forms, but physicists have narrowed the most influential to that of turbulence, atmospheric absorption, and scattering (Perram et al., 2010). These atmospheric effects can significantly degrade a laser beam, sometimes diminishing all of its intensity by mid-propagation, keeping it from reaching its intended target.

To mitigate the effect of atmospheric interferences, three key considerations are made: select laser designs with power, wavelength, aperture, and beam quality settings which best propagate through the atmosphere; determine ideal engagement geometries between the aircraft and the target; improve predictive laser system

performance abilities by developing a process which models atmospheric variations that emulate relevant environments for testing or operations.

To determine the best performing HEL weapon system designs and engagement geometries for atmospheric propagation, there must be a method to objectively capture, compare, and isolate the effects of the system's performance parameters despite atmospheric influences being present. Current HEL modeling and test practices have documented very little on this concept. Isolation of cause and effect relationships becomes more difficult when random, uncontrolled, varying parameters exist which vary performance outcomes. Having random variables in any test can degrade performance, or some cases enhance performance, making it hard to differentiate between a performance outcome due to interferences, parameter settings, or a combination of both. Design of Experiments and Response Surface Methodology are two statistical techniques appropriate to track traceability between cause and effect relationships of an outcome. These two methodologies are incorporated in this research.

1.11 Introduction to High Energy Lasers

Laser development started back in the early 60's. "Laser" comes from the acronym Light Amplification by Stimulated Emission of Radiation (LASER). Stimulated emission occurs when light or electricity is pumped into a lasing medium which excites atoms, causing them to lose an electron. The electron is pumped into a higher state, and when it drops back down to its ground state, it emits a photon, creating a coherent electro-magnetic energy. The photons are channeled through a beam control system and focused onto a spot which projects a consolidated and tight laser beam through a beam director, which focuses and magnifies the intensity of the beam as it exits the laser weapon system. By Department of Defense classification, a high powered laser is one in which the output power exceeds 25 kilowatts (Anderberg and Wolbursht, 1992). The output intensity of a laser depends on several factors, such as the laser weapon's sub-system configuration and characteristics. Laser weapons typically have four sub-systems: beam control, the laser itself, system control, and thermal management. Some of the characteristics of a laser

weapon are its wavelength, power level, aperture mirror size, and beam quality. All of these factors play a role in the intensity of output power. The most common types of lasers built today are COIL, Fiber, Free Electron, and Solid State. Aside from sub-system design differences, the primary difference in the performance of these laser types is attributed to differences in laser beam wavelengths.

If successfully designed, engineered, tested, and deployed, HEL weapon systems could be highly efficient in defending against or attacking a large class of target types, provided sufficient atmospheric conditions exist. HEL weapons have the potential to hit targets beyond the range of any Air-to-Air or Air-to-Ground weapon in inventory to date. No other weapon can travel at the speed of light, with ultra-precision strike capabilities, then immediately re-target and engage another target, all with having no signature trace, and executed with minimal collateral damage. Unlike conventional weapons, HEL weapons can have an unlimited magazine, enabling it to fire for long durations. When deployed in the field, the hope is HEL weapon systems will defend against UAVs, cruise missiles, aircraft, optics/sensors, ballistic missiles, and surface-to-air munitions (Souder and Langille, 2004). Having an airborne weapon of this caliber would change air warfare.

1.12 High Energy Laser Performance Modeling

There are three primary HEL scaling law codes used by the Air Force Research Lab's Directed Energy Directorate for modeling laser propagation for laser to target Air-to-Air, Air-to-Ground, and Ground-to-Ground engagement scenarios. These codes are the High-Energy Laser Consolidating Modeling Engagement Simulation (HELCOMES), High Energy Laser End-to-End Operational Simulation (HELEEOS), and Scaling for HEL and Relay engagement (SHaRE). Each is anchored to wave-optics codes, which are based on actual collected atmospheric observations and very high fidelity physics models. These scaling codes are all system-level codes, which means sub-system components (beam control, thermal management, etc.) are not modeled. The models only capture the laser beam as it leaves the aperture mirror and propagates through the atmosphere. The codes calculate a variety of outputs, one of which is the intensity, or irradiance (watts/cm^2)

delivered on a spot. Irradiance, discussed in section 2.15, is a function of the user-defined inputs for the laser characteristics as well as any nuisance factors that reduce the intensity of the beam as it propagates. Analysts take irradiance outputs from the HEL scaling codes and compare them to actual target vulnerability criteria, enabling them to equate irradiance to an achieved level of damage to a target. Although the scaling codes are not as accurate as the wave optics codes, (by approximately +/- 10%), they are faster, and less complicated to use than wave optics codes, making it more convenient for running large trade-space analysis with multiple scenarios and getting results quickly. The scaling code used for this thesis is HELEEOS 3.0, which is discussed in section 2.14.

1.13 Current High Energy Laser Test Practices

HEL tests conducted by the Air Force Research Lab's Directed Energy Directorate consist of Ground-to-Ground scenarios using a horizontal path propagation. Typically these laser-to-target engagements are at fairly short engagement distances (i.e., <2 miles). After looking through previous DE program test evaluation master plans, it does not appear that a design of experiment (DOE) methodology has been employed. This thesis demonstrates the benefits gained by applying DOE to both HEL modeling, and by inference, designing a live test.

1.2 Problem Statement

The problem addressed in this thesis decomposes into two sub-problems.

Sub-Problem 1: Limitations of current HEL engagement models. The HEL performance models currently used by the DoD Modeling & Simulation community are very capable and useful in the conceptual design phase of an HEL weapon system. However, they are all deterministic, which assumes away all variations and experimental error that would be present in any real test demonstration.

Sub-Problem 2: The absence of DOE application in current airborne HEL Testing. Although there have been air-to-ground test demonstrations where airborne HEL weapons have achieved desired damage to targets, there has not been extensive application or analysis using DOE methodology. Without the application of DOE

techniques, such as use of replications, random order combinations, and blocking techniques, test design may not capture the full spectrum of valuable information which could be extracted from each test, such as insights to performance improvements. Tests can be expensive, with limited range time and human resources, thus it is important each test be strategically planned with a purpose and efficiency. In addition, without use of DOE, there is an increased probability of introducing a systematic bias and/or experimental error caused by the experimental sequence itself, making it impossible to distinguish between impacts caused by random error and those of the actual system.

1.3 Problem Approach and Scope

Since it is not possible to conduct actual airborne HEL testing to support this thesis, modeling and simulation is used. The scenario modeled for this research is an Air-to-Ground HEL engagement between an airborne B1-B aircraft and a truck, set in the 2022 timeframe. Two models are used to simulate this engagement, an atmospheric model called Laser Environmental Effects Definition and Reference (LEEDR) , and the HELEEOS HEL propagation model. Typical modelers of HEL engagements use HEL engagement models as an all-in-one model, letting the model calculate its own atmospheric effects via algorithms for turbulence and extinction. Algorithms are an excellent way to supplement for not having actual atmospheric data, allow for the models to run quickly, and provide a rough idea of HEL performance for large trade-studies with the objective to compare system designs. However, a major disadvantage to using algorithms is that all outputs of HELEEOS as a stand-alone model are deterministic. This means the atmosphere remains constant among runs; there are no random variations modeled in the atmosphere. To incorporate varying atmospheric conditions, LEEDR, an atmospheric model, is used in conjunction with HELEEOS. LEEDR takes actual atmospheric observations from a geographic location on the earth's surface and then interpolates and outputs atmospheric conditions for the troposphere and stratosphere. These atmospheric conditions are output into an excel file, which reflects a snapshot of the atmosphere at a specific time. This profile is then imported into HELEEOS. In order for each run

of HELEEOS to have a different atmospheric snapshot, a new LEEDR profile is created and imported for each run. Figure 1 displays the process used to model atmospheric variations in the Air-to-Ground Engagement.

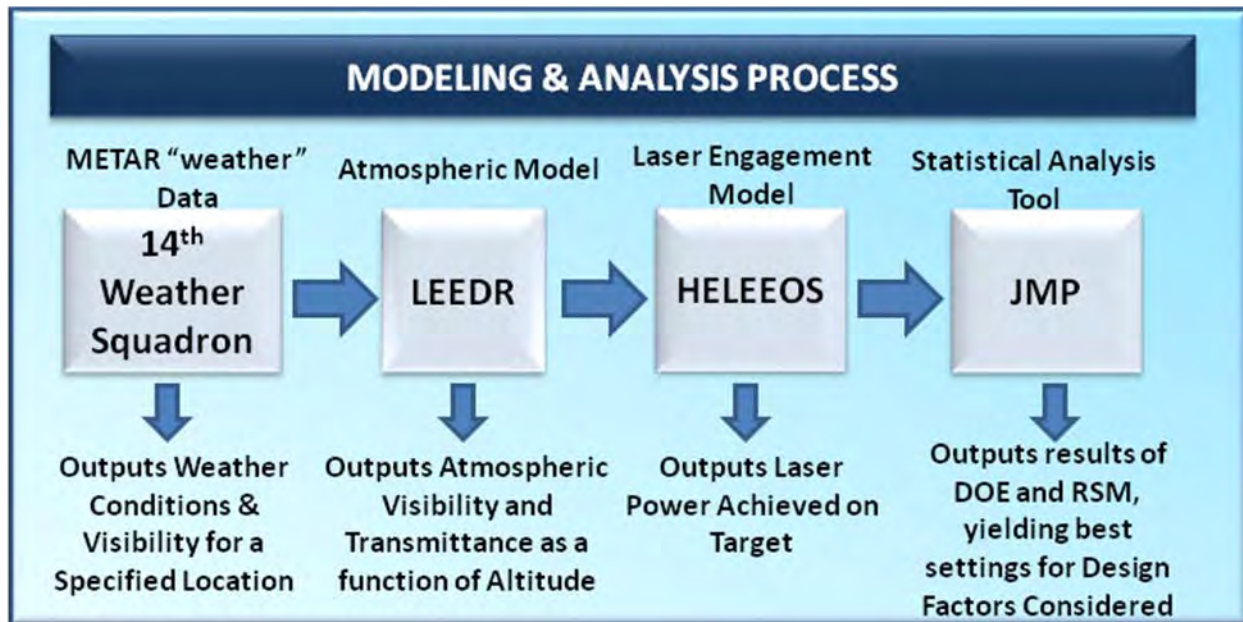


Figure 1: Model Process for an Air-to-Ground HEL Engagement Model

Reflecting actual variations in weather conditions is important for accurate modeling of a real life HEL engagement scenario or test demonstration. In practice, the atmosphere will change, and our performance changes as a result.

Design of experiments and Response Surface Methodology are two statistical approaches used in this research. DOE has recently been introduced into the test and evaluation community, however there is little evidence of use in Directed Energy testing, or even Directed Energy HEL modeling. DOE methods establish test a design which enables tractability between cause and effect relationships of results captured. Without the use of DOE, nuisance factors present may limit one's ability to interpret the contribution each parameter has towards engagement performance. Response Surface Methodology examines the surface of interactions between parameters, enabling analyst to determine the best settings for a system design,

minimize the variance caused by nuisance factors we cannot control, and overall increase probability of achieving the desired intensity on target. JMP is the statistical tool used in this work.

1.31 Objectives

1. Introduce atmospheric variability to a pre-existing HEL scaling model to make it representative of a live HEL test. Atmospheric variability, a known nuisance factor, will dilute the traceability of the impact caused by controlled factors in the test.
2. Apply Design of Experiment (DOE) methodology to create an experimental design that will enable one to isolate the effects of the controlled parameters, despite error and nuisance factors present.
3. Apply Response Surface Methodology (RSM) to determine best settings for an experimental design, and extend the significance of that design to the Air-to-Ground mission scenario defined in section 3.2.

1.32 Assumptions

Many assumptions have been made to frame this research. Realistically, there are existing sub-system design and integration complexities still to overcome with airborne HEL weapon systems; however they are not addressed in this thesis. This research assumes full technology maturity for all system designs conceived, even though that is not the case. The laser weapon system designs considered for this research are presumed to exist in a 2022 timeframe. This thesis is based upon modeling and simulation only.

1.4 Thesis Overview

Chapter 2, Background and Literature Review, provides an introduction to pertinent concepts and terminology applied and referenced throughout this thesis. Addressed are fundamental theories of the atmosphere, atmospheric and laser engagement model capabilities, an introduction to DOE and RSM, and a brief overview of previous case studies in related research. Chapter 3, Research

Methodology, takes the methodologies discussed in chapter two and applies them to an Air-to-Ground laser engagement scenario modeled for this research. This chapter discusses the development of an experimental design, implementation of model modifications to add atmospheric variability, model interactions, and method in which data inputs and outputs were strategically determined in a pre-planning phase. Chapter 4, Results and Analysis, takes the results of the DOE produced using HELEEOS, and interprets the statistical significance of the response as a function of the design factors. Chapter 5 concludes this thesis and takes the results from Chapter 4 and extends them to a broader application of how DOE could be incorporated into Directed Energy modeling and simulation, as well as testing. Chapter 5 also provides recommendations for future research.

II. Background & Literature Review

This chapter introduces literature, concepts, and terminology related to the areas used to either describe, explain, or solve the problem scenario in this thesis. Atmospheric modeling, HEL engagement and lethality models, DOE, and RSM are the areas discussed throughout this thesis. Background on these concepts is important for comprehension in succeeding chapters. Case studies on HEL modeling and analysis are also discussed to provide reference and insights from similar studies to this research.

2.1 Theories of the Statistical Atmosphere

Despite how efficient and well designed laser weapon technology becomes in the future, performance will always have a dependency on atmospheric conditions, an uncontrolled factor. Most atmospheric effects are likely to have adverse influence on beam path propagation. Inability to propagate through poor atmospheric conditions is why “all weather weapon” does not apply to HEL weapons. Because of this, it is usually assumed that lasers will be used in combination with other weapons, rather than as a stand-alone offense or defense. Interaction effects that exist between laser beams and the atmosphere have been researched extensively, and several books have been published on this topic alone.

Light cannot propagate unless it has a medium through which it can transmit. For laser beam path propagation, the atmosphere is the medium, and the transmission varies through each layer of the atmosphere. The interaction between the laser and atmosphere is at a molecular level. The different types of interactions are due in part from temperature differentials encountered when traveling through a dynamic atmosphere. “In terms of total mass and effects on laser weapon systems, the two most important layers of the atmosphere are the troposphere and stratosphere” (Perram et al., 2010). Figure 2 below displays the complex layers of the atmosphere and classification by altitude and temperature.

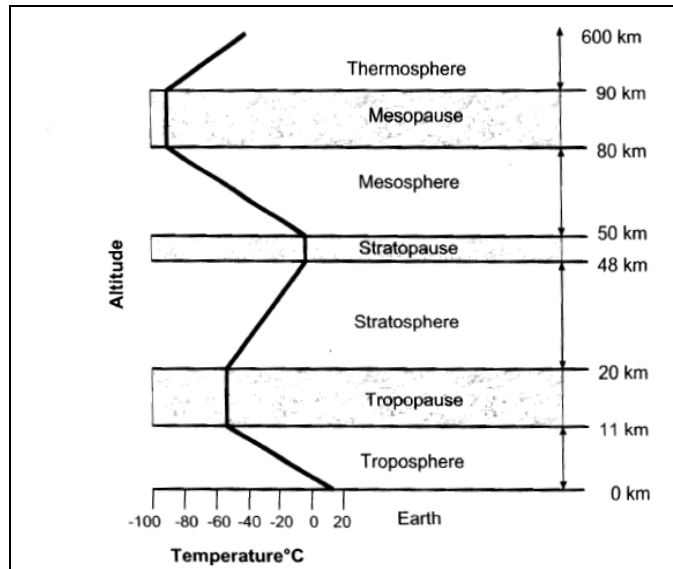


Figure 2: Diagram Depicting Various Atmospheric Layers and Air Temperature (Andrews and Phillips, 2005)

The troposphere is the lowest portion of the earth's atmosphere, from 0-11 km in altitude, and contains the majority of weather. This layer is harshest on laser beam propagation, and is often called the "muck" of the atmosphere. Since passing through this region is necessary for Air-to-Ground and Ground-to-Air engagements, it is key to make the slant range through this atmospheric layer as short as possible, i.e. the platform and target 90° above or below the other. The stratosphere is the layer above the troposphere, 20-40 km in altitude, and because of solar radiation, temperatures increase with altitude. Temperature, air density, water vapors, and pressure all change from day-to-day, creating different conditions in the layers of the atmosphere at any given point in time. Since laser performance is highly dependent on these conditions, it is important to understand laser performance not only in good atmospheric conditions, but also in bad.

Out of all factors that exist in the atmosphere, only a few phenomena have been specifically tied to having a significant influence on laser beam propagation. Most atmospheric effects on laser weapon can be traced to three atmospheric phenomena: absorption and scattering, (collectively referred to as extinction), and

turbulence. These phenomena listed are discussed below, as well as their effects incorporated into the Air-to-Ground HEL engagement modeled for this research.

2.11 Extinction

Extinction is the loss of electro-magnetic energy (i.e. laser wavelengths) along a path through a medium due to absorption and scattering. Losses due to all effects is attenuation. Extinction is the term used to characterize both effects of absorption and scattering, which are both measured in terms of percent transmittance through the atmosphere, relative to transmittance through a vacuum.

Absorption refers to water vapor or gas molecules in the atmosphere, which absorb heat as photons pass through them. “Transitions that occur within absorbing molecules result in molecular collisions...[making] the medium gain thermal energy” (Perram et al., 2010). This reaction causes the atmosphere to heat up. Since the troposphere contains 99% of all water vapor, it has the greatest amount of absorption. Seasons and time of day also influence absorption. The effect of laser transmission caused by absorption, T_{abs} , can be calculated using equation 1.

Absorption is a function of wavelength, λ , transmittance intensity with absorption, $I_{tA}(\lambda)$, transmittance intensity in a vacuum, $I_0(\lambda)$, the absorption cross sectional area in m^2 , σ_{abs} , and the absorber number concentration in m^{-3} along the transmission path, N_z , (Perram et al., 2010):

$$T_{abs} = \frac{I_{tA}(\lambda)}{I_0(\lambda)} = e^{\sigma_{abs}(\lambda)N_z} \quad (1)$$

The primary issue with absorption is a non-linear effect called thermal blooming. This effect produces changes in air density, sometimes warping the beam into a crescent shape, decreasing the intensity of the center of the beam. Thermal blooming is highly dependent on wavelength. “Absorption by O_2 and O_3 essentially eliminates propagation of radiation at wavelengths below 0.2um, but there is very little absorption at the visible wavelengths (0.4 to 0.7 um)” (Andrews and Phillips, 2005). When selecting a laser design and geometry, it is important to understand atmospheric effects and design a scenario to circumvent the likelihood of those

effects influencing performance. Thermal blooming has been shown to “increase with higher laser power, higher absorption, longer range to target, smaller (more focused spot size, and lower wind speed or slow slew rates” (Perram et al., 2010)). This knowledge can be useful when choosing particular power levels, ranges, wavelengths, and spot sizes to circumvent the effects of absorption.

The other type of extinction is atmospheric scattering. “Scattering of electromagnetic waves in the visible and IR wavelengths occurs when the radiation propagates through certain air molecules and particles” (Andrews and Phillips, 2005). There are two types of scattering, Rayleigh’s molecular scattering caused by laser photons being larger than the air molecules, and “Mie’s aerosol scattering, which is scattering caused by laser photons being smaller than particles” (Andrews and Phillips, 2005). The effect of laser transmission due to scattering, T_{sca} , can be calculated using equation 2. Scattering is a function of wavelength, λ , transmittance intensity of scattering, $I_{ts}(\lambda)$, transmittance intensity within a vacuum, $I_0(\lambda)$, the transmission path, z , and the scattering coefficient, α_s , (Perram et al., 2010):

$$T_{sca} = \frac{I_{ts}(\lambda)}{I_0(\lambda)} = e^{-\alpha_s z} \quad (2)$$

2.12 Turbulence

Turbulence, denoted C^n_2 , is a result of random temperature differentials between the earth’s surface and the atmosphere. Daytime temperatures produce negative temperature gradients, which bend light rays upward, and night temperatures produce positive temperature gradients, which bend light downward (Andrews and Phillips, 2005). These fluctuations produce variations in the speed in which wavelength propagates (refractive index), and cause wave front distortions in the atmosphere affecting the phase of light when a laser beam passes through it. Refractive index is based upon the speed at which a wavelength propagates through the atmosphere, in comparison to the speed at which light travels. Light that passes through a vacuum would have an index refraction of 1. As a wavelength approaches the earth in a Air-to-Ground scenario, it will decrease in speed. Ideally, the

atmosphere would be like a vacuum, homogeneous, with no variations, allowing a beam to propagate without any loss of intensity. We use the term diffraction limited to describe such a beam with no degraded effects. Figure 3 shows a comparison of a diffraction limited beam to that of a degraded beam passing through the atmosphere. The downward and upward gradients shift light.

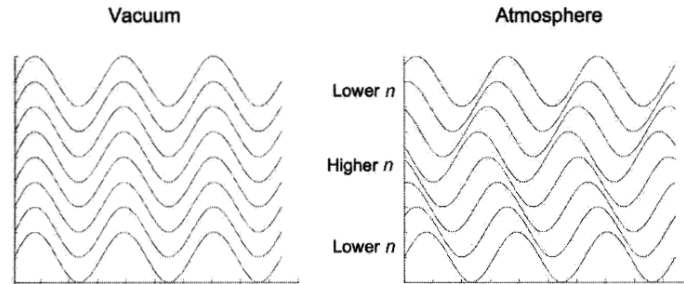


Figure 3: Example of How Variations in Refractive Index Affect Phase of Light. Note that a lower n implies faster propagation speed (Perram et al., 2010)

Other distortions caused by turbulence include aberrations, scintillation, loss of spatial coherence, beam defocus, or beam spread, all of which could drastically degrade a propagating beam, thus also its intensity on a target. Figure 4 depicts the distortions turbulence has on a beam. The circular patterns in the second illustration of Figure 4 represent turbulent eddies, caused by density variations. These density fluctuations have an adverse effect on laser propagation.

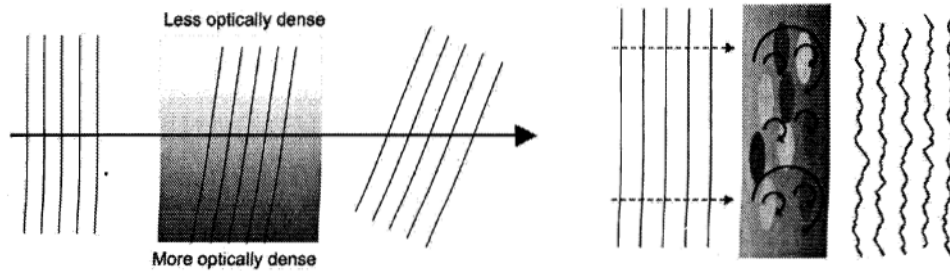


Figure 4: Example of How Turbulence Effects the Wavefront of Electromagnetic Energy (Perram et al., 2010)

Overall turbulence and scattering effects can be reduced by selecting appropriate laser wavelengths. These effects are incorporated into the Air-to-Ground engagement models used for this research, discussed in the following sections.

These effects are important to model, since understanding the way laser beams propagate and interact with atmospheric molecules may give insights to HEL weapon system performance enhancements.

2.13 Atmospheric Models – LEEDR

LEEDR was developed by the Air Force Institute of Technology Center for Directed Energy (AFIT/CDE). It incorporates first principles atmospheric propagation and uses upper air data to characterize percentages of molecular and aerosol absorption, scattering, and turbulence. Specifically, LEEDR calculates and outputs four categories of data: path transmittance, path extinction (km^{-1}), surface visibility (km), and slant path visibility (km). LEEDR can also model the effect of clouds, fog, and rain. This model was specifically developed for modeling atmospheric effects for lasers propagation, which is why each atmospheric profile is a function of a specified laser wavelength. LEEDR creates “profiles of temperature, pressure, water vapor content, optical turbulence, and atmospheric particulates and hydrometeors as they relate to line-by-line layer extinction coefficient magnitude at wavelengths from the UV to the RF” (Fiorino, 2008). LEEDR can model multiple sites all around the world, and for several different seasons. Figure 5 provides a screen shot from LEEDR with dots indicating the available geographic locations in the model.

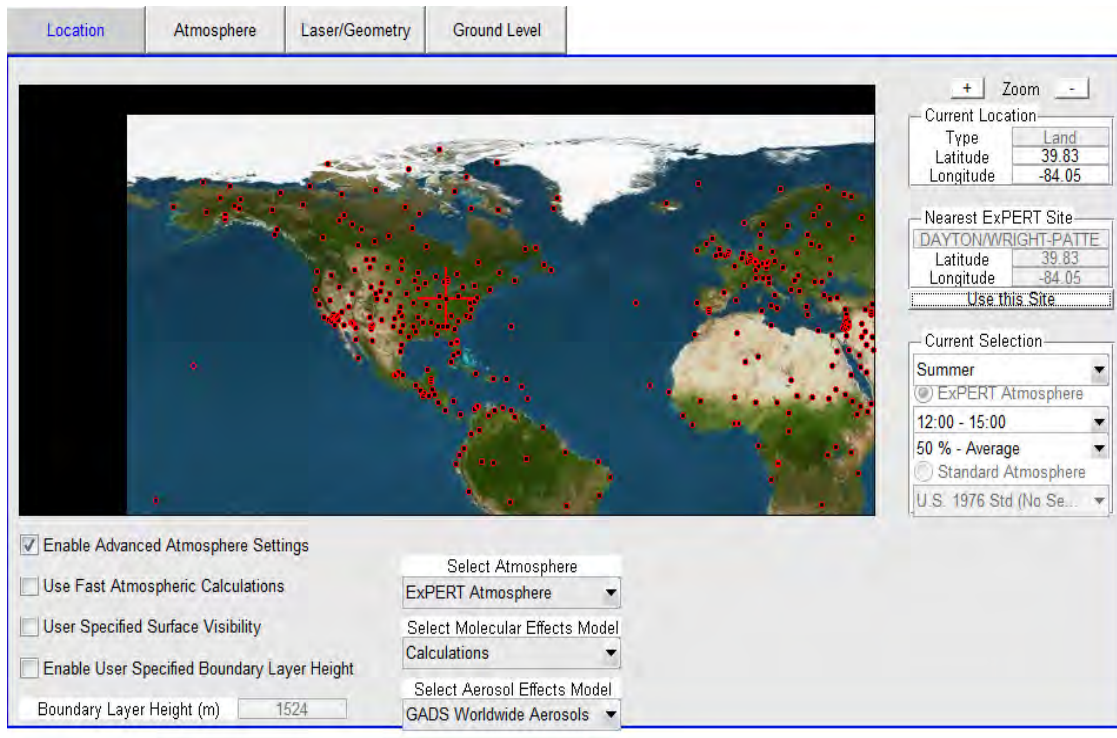


Figure 5: LEEDR Geographic Locations

LEEDR calls on databases, such as Extreme and Percentile Environmental Reference Tables (ExPERT), the Master Database for Optical Turbulence Research in Support of the Airborne Laser, and the Global Aerosol Data Set (GADS) to acquire probability density function data for the geographic location selected, enabling the upper air to be assessed for absorption, scattering, turbulence, and other parameters. In relation to how they are calculated, molecular scattering is computed based on Rayleigh theory, molecular absorption effects are computed for the top 13 absorbing species using line strength information from the HITRAN 2004 database in conjunction with a community standard molecular absorption continuum code, and aerosol scattering and absorption are computed with the Wiscombe Mie model (Fiorino, 2008).

Although LEEDR can reference databases on file to acquire information on specific geographic locations, it also provides the option to take user inputs for a geographic location, (i.e. temperature, dew point, pressure, and relative humidity) and calculate upper air conditions based on those inputs. Each profile is dependent

on the laser wavelength defined by the user. The option to input data is extremely useful, particularly when wanting to capture atmospheric variations seen in one location over a period of time, or season rather than averaged observations provided by ExPERT. This thesis utilizes the user-input option to simulate varying atmospheric conditions.

2.14 HEL Scaling Model – HELEEOS

Scaling codes are considered to be moderate in accuracy in comparison to higher fidelity wave optics codes that are based on microscopic laws of electromagnetic (E-M) radiation. “[HEL] Scaling codes start from phenomenology of and analytical approximations to the E-M wave equations, and attempt to represent the details of propagation through the atmosphere with a few parameters based on integrated properties of the atmospheric conditions, light intensity, wavelength, etc.” (Rockower, 1985).

HELEEOS is a system- level scaling code that models various HEL engagement scenarios, modeling the propagation the beam from the laser source to its target. HELEEOS was developed by the AFIT Center for Directed Energy and is anchored to high fidelity wave-optics code, called WaveTrain. It models everything from atmospheric effects like absorption, scattering, and turbulence, to fog, rain, and clouds. HELEEOS can model many types of engagement scenarios, such as Air-to-Ground, Ground-to-Air, and horizontal path propagation. HELEEOS is integrated with LEEDR, which allows it to access a climatologically database for numerous geographic locations worldwide. Forty years worth of weather observations for geographic locations are included in the ExPERT database, which are averaged and available for scaling codes to reference. Absorption and scattering transmission numbers are calculated based on the atmospheric characteristics of the geographic location selected within HELEEOS. HELEEOS takes absorption, scattering, and turbulence effects and calculates a vertical profile by which laser transmittance can be estimated.

User inputs include engagement scenario geometry, laser, optics, and platform characteristics, atmospheric conditions, and target information. HELEEOS

calculates a variety of outputs about the engagement, ranging from a detailed list of atmospheric effects, peak and average intensity on target, power in bucket, etc. It is a very effective tool for running large performance trade studies to identify key performance parameters. Many analysts use HELEEOS as the first stage of analyzing a large trade space of designs, then once they scope it to something more manageable, they use wave optics to gain higher fidelity on the designs of most interest.

2.15 Target Lethality Modeling

HEL performance measures typically relate target lethality, or damage criteria. “Damage” is subject to interpretation, but may can be defined as achieving a target capsize, explosion, or simply damaging the target enough to render it non-functional. Since materials melt at different rates and require different intensities, most target types will have their own target lethality requirements. “The desired effect on the target ultimately decides what is needed from the laser” (Anderberg and Wolbarsht, 1992). Since the objective is to damage a target, the HEL beam is focused on the region of weakest strength on the target. Even different aim-points on one target will have different lethality criteria, based on differences in material strength.

Three common performance measures used to HEL intensity on target are irradiance, bucket size, and fluence.

Irradiance, I , refers to the HEL power, P , delivered on a target, divided by the area of the beam, A . Its units are in watts/cm², or power per unit area:

$$I = \frac{P}{A} \quad (3)$$

Irradiance in combination with lase time on target is called fluence. Fluence, F , is irradiance accumulated on target over a specific time frame, or dwell time, τ_D . Its units are in kilo jewel /cm2, or energy per unit area:

$$F = I\tau_D = \frac{P\tau_D}{A} = \frac{P\tau_D}{\pi w_0^2} = P\tau_D \left(\frac{\pi D^2}{4R^2\lambda^2} \right) \quad (4)$$

Fluence is the most accurate measure to determine if a HEL weapon will achieve a certain level of damage to target. Fluence requirements by aim-point reflect a target's vulnerabilities and susceptibility to HEL attack. For this reason, fluence levels are kept classified, and unclassified measures, like irradiance and power in bucket are used for conducting unclassified analysis.

Power in Bucket, *PIB*, is the total power (in Watts) delivered to a specifically defined spatial region, typically circular or square, on the target. It is used as a measure of the total power delivered in the defined area. However, any information on the specific spatial distribution (very peaky, or very broad, or very broken/distorted) of power delivered is lost with this metric.

For convenience, analyst use irradiance as the measure to compare HEL concepts, as it provides a basis to compare two concepts for achieved power per unit, yet does not reveal sensitive information about its target's vulnerabilities. This thesis uses power in bucket as its performance measure.

2.16 JMP Statistical Tool

JMP is a statistical tool developed by SAS in 1989. JMP is extremely useful for developing custom experimental designs, and performing regression analysis to fit an empirical model. The tool has a multiple number of transformations and techniques use to best fit and evaluate an empirical model. JMP is the tool used to conduct statistical analysis in this research.

2.2 Design of Experiment

DOE is a methodology used to plan, conduct, and analyze an experiment. "It is the process of planning the experiment so that appropriate data will be collected and analyzed by statistical methods, resulting in valid and objective conclusions" (Montgomery, 2009).

2.21 Terminology

There are many terms used throughout this thesis in which the reader should be somewhat familiar. A response variable is selected by the experimenter, and is the output from a system, or the result collected from an experiment. There can be many responses of interest collected during in an experiment, but they must be observable and measurable. A factor is a parameter or “input” that needs to be set for an experiment. Factors can be classified as controlled or uncontrolled. As the term suggests, controlled factors are those in which experimenter has full ability to control. An example of this may be the ratio of chemicals used in an experiment. Controlled parameters can either be held-constant throughout the entire experiment, or selected to be design factors which are intentionally varied from test to test in order to observe the impact they have on the response. If a design factor is varied, its different settings are called levels. Uncontrolled factors cause variation in the response not explained by the design factors, and are generally unavoidable, yet present in any test. They are also known as nuisance factors, noise, or error. Examples of this may be influences of weather, use of non-homogenous test materials, poor instrument calibration, operator error, etc. Some nuisance factors have little to no impact on the response, however some can have a significant impact, transmitting variations to test results which dilute the traceability of the cause and effect relationship between the design factors of interest. The ratio of impact caused by design factors and those caused by nuisance factors is often referred to as the signal-to-noise ratio. A treatment combination or design point is a unique combination of factors and their levels to be tested. An experimental design is the actual schedule indicating which order the design points will be run.

2.22 Seven Stages of Design of Experiment

Douglas Montgomery, author of a leading DOE text, suggests using seven stages of DOE methodology. These seven stages of DOE are important to creating an effective and efficient test from which objective conclusions can be drawn.

- 1) ***State the Problem and Objective***. This stage defines the problem or need to

have the test in the first place. It usually involves speaking with customers to understand expectations and clarify test objectives.

2) *Select appropriate response variables.* A test may have multiple response variables. It is key they are measurable, and reflect important or valuable information about the design factors being tested.

3) *Select design factors, and number of levels and ranges to be varied.* Design factors are typically chosen based on the belief they will effect system performance. The number of levels a design factor varies is based on sensitivities, or the rule of thumb that levels be far enough apart that a standard deviation of three is seen in the response distribution. The range of a design factor is based on the size of design space one wishes to analyze.

4) *Select an Experimental Design* – There are two key principles Montgomery stresses when creating an effective and efficient experimental design, and they are replications and randomization.

Replications are independent repeats of a factor combination. The advantages of replications are that they provide more than one sample point of a treatment combination, which will yield a better estimate of pure error, as well a better estimate of the true population mean and variance. Replications also provide a basis to objectively compare two sets of data to see if they are statistically different.

Randomization is the principle by which we can assume error is independent and identically distributed across the experiment. Randomization is both a technique and statistical assumption in DOE. The technique of randomization typically applies to intentionally randomizing the order in which a test of treatment levels will be run. This technique comes from the statistical assumption that error, if present, is a random variable which is identical and normally distributed. This means if error is present, it is best spread randomly across all tests as opposed to systematically spread, which can bias results. This assumption is significant because it allows us to draw unbiased, statistical inferences about our data.

There are many types of experimental design, such as factorial, fractional factorial, Latin least square, etc. No one design can best accommodate every type of

test scenario, which is why there are multiple types of designs. The design used in this research is a factorial design, which varies each design factor in conjunction with other factors to enable an assessment of interactions, if they exist.

5. Conduct the test.

6. Statistical Analysis of the Response. The objective of statistical analysis is to analyze the response variables and try to explain variations produced by the regressor variables (design factors) of interest. The analysis process begins by developing an empirical model built from the response data. Figure 6 shows the relationship between the real system, the observations produced from the system, and the empirical built from the observations which allows us to draw inferences back to the real system. This diagram is presented by AFIT's Dr Raymond Hill in OPER 688, Design of Experiments. This process assumes Montgomery's seven stages of DOE are followed.

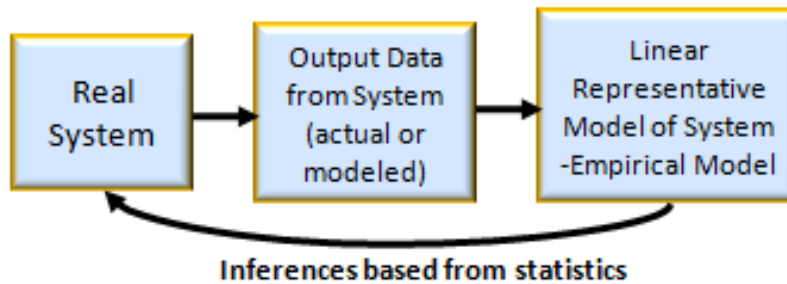


Figure 6: Relationship of Real Systems to their Empirical Models

Output data from a system is considered a sample of the population of all possible outputs from that system. The more samples obtained, the better the estimate of the true population mean and variance, which describe the first two moments of any distribution. An empirical model is a functional representation a system, and is built on observations either produced by the system during a test, or from a simulation of the system. A well fit empirical model can provide a predictive capability for how the system performs, through the design space considered. Although empirical models may not achieve a perfect fit, particularly to non-linear data, they can provide a good approximation of system performance. An empirical

model is composed of four parts: a response variable, y , a y-intercept term, β_o , any regressor variables modeled, β_k , (where k is the number of design factors), and an error term, ε .

$$y = \beta_o + \beta_k + \varepsilon \quad (5)$$

The error term is any variation that cannot be explained by the regressor variables. As long as statistical principles are incorporated, statistical inferences can be drawn about the data, such as dependencies and parameter relationships (including those non-linear). Also, with replications included in the experimental design, sets of data points for one design factor provide a better estimate of pure error that exists in the test.

For this research, a meta-model technique is used, where an empirical model is built upon outputs of a model itself. Meta-models are used when live tests cannot be conducted or response data from previous tests are unobtainable.

5) *Conclusions and Recommendations* Empirical models and regression analysis can help reveal a great deal about cause and effect relationships between regressors and an associated response, however, the rule of causality states conclusions implying cause and effect cannot be made based on data alone, but in conjunction with other information about the system. The empirical model can suggest design factor levels and ranges which are found to be achieve the best performance, given the design space considered or modeled. This ensures conclusions are not being made just on data alone, which could be a result of coincidence, but rather supported in combination with knowledge known about how the system works, and weather statistical results make practical sense.

2.3 Response Surface Methodology

RSM is a technique used to analyze data that cannot simply be characterized by a first order empirical model. Typically RSM is used to estimate system performance over some region of interest and use that empirical model to either find factor settings that achieve improved performance or to locate new areas where improved performance might be attained. For this research RSM is used to visualize

the nonlinear relationship between our factors interest and the model response. We also use the optimization component of RSM to suggest our area of best performance in our defined design region.

2.4 Case Studies – Analysis & Results

Numerous sensitivity studies have been conducted using HEL engagement models, specifically HELEEOS. Three of these studies are discussed below:

- 1). “Capability Assessment of the High-Energy Laser Liquid Area Defense System (HELLADS)”, by Ryan Ponack. Ponack uses HELEEOS with the Extended Air Defense Simulation Model (EADSIM) mission level model, to estimate the performance a conceptual weapon system in an Air-to-Ground engagement in a homeland defense arena. Ponack found that the most influential parameters analyzed to be platform altitude, target altitude, platform velocity, and line of sight (Ponack, 2009).
- 2). “Characterizing effects and Benefits of Beam Defocus on High Energy Laser Performance Under Thermal Blooming and Turbulence Conditions for Air-to-Ground Engagements”, by Scott Long, examines the advantages of defocusing a beam with nuisance factors present. Long models the Air-to-Ground engagement in HELEEOS and verifies results with wave optics simulations (Long, 2008). Results show reasonable improvement of intensity on target with defocusing the beam. Long examines other sensitivities by varying one factor at a time.
- 3). “Assessment of Optical Turbulence Profiles Derived from Probabilistic Climatology”, by Brett Wisdom. Wisdom implements DOE, using a factorial design to statistically compare values between turbulence within HELEEOS to actual thermosonde data. He found that the two data sets are statistically equivalent, within a confidence interval of 80% (Wisdom, 2007). This helped verify that based on specific atmospheric layers analyzed, HELEEOS accurately simulates true turbulence effects.

Each of the above studies helps verify the accuracy of calculations within HELEEOS, and helps ensure its algorithms for calculating nuisance factors are accurate, or that it is well anchored to the high fidelity wave-optics simulations to

which it is compared. The first two case studies vary one factor at a time to capture performance sensitivities. This approach is beneficial when just estimates of main effects are of interest. However, to capture the interaction or non-linear effects within a model, two or more factors must be varied in combination. The third case study does this. All three case studies model nuisance factors using data within HELEEOS, which results in deterministic modeling of nuisance factors as a function of time of day and geographic location selected.

This thesis focuses on capturing two important aspects of modeling a realistic Air-to-Ground HEL engagement. First, an experimental design is used, which varies all factors systematically, allowing interactions and non-linear effects to be analyzed. Second, nuisance factors are modeled stochastically, and then incorporated into HELEEOS, capturing the realistic nature of a dynamic atmosphere. These two approaches allow us to draw inferences about significant effects that drive HEL performance, with respect to performance degradation due to nuisance factors present.

III. Research Methodology

3.1 Chapter Overview

This research uses DOE and RSM. DOE involves the pre-planning for determining what will be the test objective, what will vary from test to test, and how the objective will be measured. The engagement modeled is a HEL weapon deployed on a B1, attempting to immobilize a truck from an altitude of 30,000 ft. A set of 108 design points are tested (each is a simulation configuration), covering the design space for the Air-to-Ground HEL engagement scenario. These 108 design points are run through LEEDR, the atmospheric model, and HELEEOS, the laser propagation model. RSM is used to conduct statistical analysis on the response outputs from HELEEOS by using the statistical tool, JMP. This chapter discusses the modeling approach used, model limitations, inputs and work-arounds, as well as assumptions made regarding modeling simplifications. This section also discusses the how to find design settings to achieve best laser weapon performance for the design space considered.

3.2 Context of the problem

A challenge in laser weapon systems is maintaining the intensity of the laser beam from the laser source to its intended target. Interferences such as line-of-sight obstacles or the atmosphere dilute the beam's intensity. A myriad of effects influence laser weapon irradiance. A fishbone diagram in Figure 7 captures many (but not all) effects that exist in Air-to-Ground laser engagements. Fishbone diagrams are effective for understanding, scoping, and deciding how to model the problem scenario. Some of the results we measure in laser testing are irradiance, fluence, power in bucket, or other parameters which can relate information about target damage.

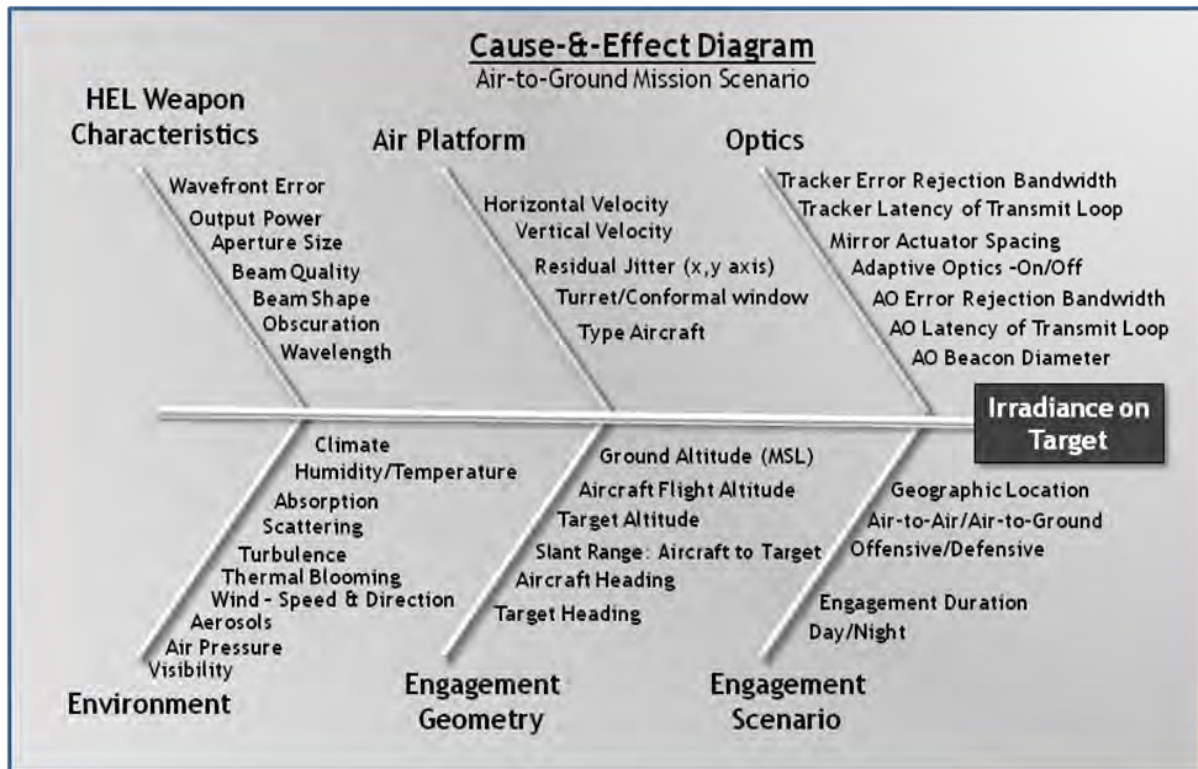


Figure 7: Fishbone Diagram Showing Factor Influences

The objective of our engagement model is to first, accurately model the Air-to-Ground engagement, and second, to capture the main effects or factors that are driving system performance. Deciding which main effects to intentionally vary for tests, or design factors, is a part of DOE methodology. The design factors are all controlled factors. Since nuisance factors exist in real testing, it is important to incorporate their effects into the modeling process, in order to collect data representative of the actual system modeled. Figure 8 updates the fishbone analysis and characterizes the effects in the problem scenario as either uncontrolled or controlled. This characterization influences the design of the research experiment.

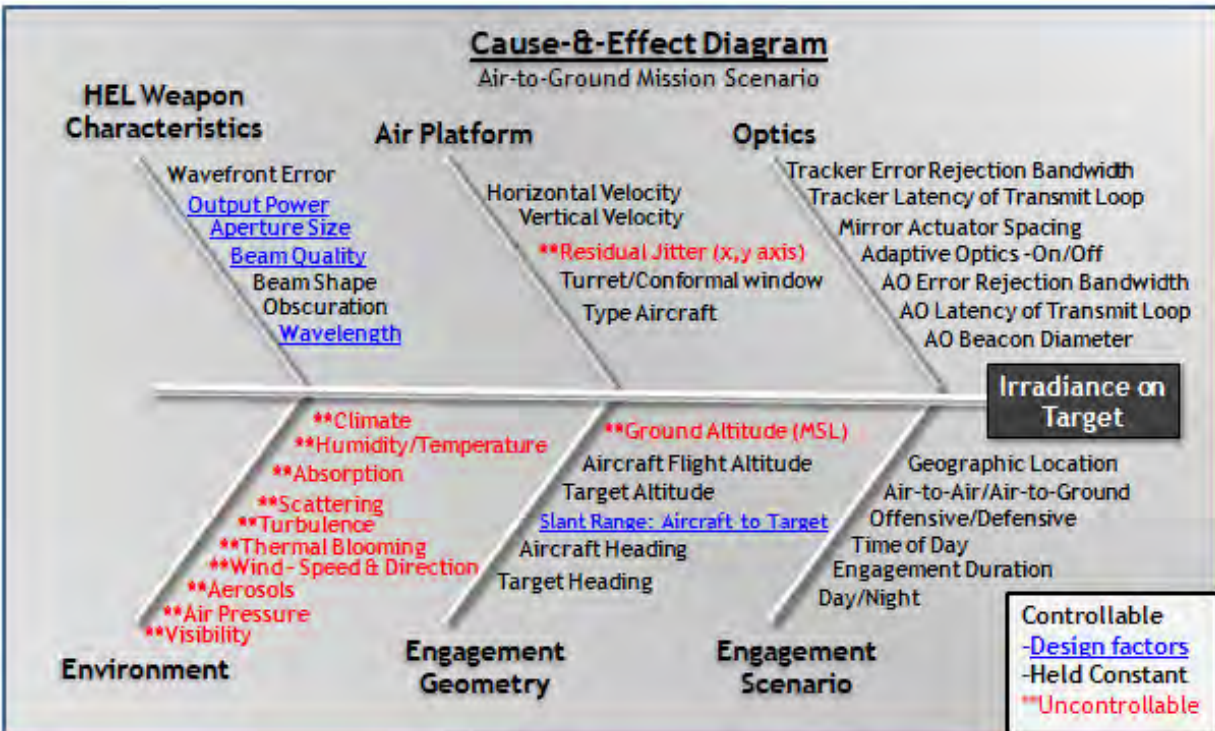


Figure 8: Fishbone Diagram Characterizing Factors

3.3 Modeling Assumptions

Several assumptions were made to reduce the complexity of the scenario being modeled. These assumptions pertain to technology maturity, system level modeling only, reduction in nuisance factor considerations, and assuming a conformal window to eliminate air vehicle aero-optical effects.

Technology Readiness Level (TRL): It is assumed that any laser weapon conceived (i.e. 400kW class electric laser with excellent beam quality), is technologically mature enough to complete the Air-to-Ground engagement being modeled. The scenario engagement is defined with a 2022 timeframe in mind.

System Level Modeling: Laser weapon sub-systems are not modeled. What is modeled is the system level, which is a fully functional laser weapon system integrated within a B1-B platform. HEL weapons are composed of four different sub-systems: thermal management, beam control, the laser itself, and system control. There are many designs and ways to configure these 4 sub-systems, each of which

can drastically alter system performance. This research models sub-system capabilities at the system level effect only.

Nuisance Factor Considerations: There are a plethora of nuisance factors in a real Air-to-Ground test scenario but not modeled in this thesis. They pertain mostly to human-in-the-loop and system nuisance factors. Human-in-the-loop nuisance factors are caused by all humans that play a part in a test and may accidentally cause slight variations from test to test, introducing inconsistencies in results. These inconsistencies could be caused by having more than one flight operator, each with different levels of experience or tendencies. Inconsistencies could be introduced by test crews with instrument calibration inconsistencies, or using different materials from test to test. An example system-level nuisance factor is residual heat left over from lasing on a test impacting a subsequent test. This introduces dependencies among tests and can bias the results of the test. The only system-level nuisance factor modeled is residual platform jitter, which are the vibrations within the platform of the B1-B in x, y, and z directions, caused by moving through a turbulence in the atmosphere. These platform vibrations create issues for the mirror alignment in the beam control system, and cause unwanted dithering to the laser beam when trying to focus intensity on a target.

Aero-Optical Elimination: Most current HEL programs still use turrets, a sensor that communicates with the acquisition and tracking and system control to acquire the location of a target. A low power laser, or track illuminator illuminates the target or aim-point, and then passes the high power through the turret, sending the beam propagating through the atmosphere to its target. The issues with turrets are that when deployed, they are not flush with the bottom of the aircraft, and because they protrude, they create aero-optical effects which forces air to channel around the turret. These effects can be highly detrimental to laser weapon performance, particularly when shooting to targets in the rear of the aircraft direction in flight. Conformal windows are a concept introduced which fit flush with the aircraft belly, thus reducing aero-optical effects. This type of window reduces the field of view or field of regard, as it is mostly limited to shooting straight down

when at low altitudes. For this research, a conformal window is assumed, and aero-optical effects are not modeled.

3.4 Modeling Process and Inputs

For this research, the Air-to-Ground HEL engagement scenario is modeled using one database, two models, and one statistical tool. Figure 9 shows the process used to model the engagement, produce the response data, and conduct statistical analysis. This process starts by developing a database containing Meteorological Aviation Reports (METARS) from the 14th Weather Squadron. METARS provide recordings of visibility, atmospheric extinction, and other atmospheric effects at the earth's surface for a specified geographic location. METAR observations are stored in this database and picked randomly as input to LEEDR. This induces atmospheric variation into the HEL engagement, making each model stochastic. LEEDR 3.1 takes the METAR observation and simulates weather conditions in the troposphere and stratosphere. LEEDR outputs absorption, scattering, and other atmospheric conditions as a function of altitude. These atmospheric profiles are then imported into HELEEOS 3.0, which propagates the laser through the specified atmosphere and outputs irradiance on the target. JMP is used to conduct statistical analysis on the response data and allows us to determine which factors in the model contribute most to HEL performance.

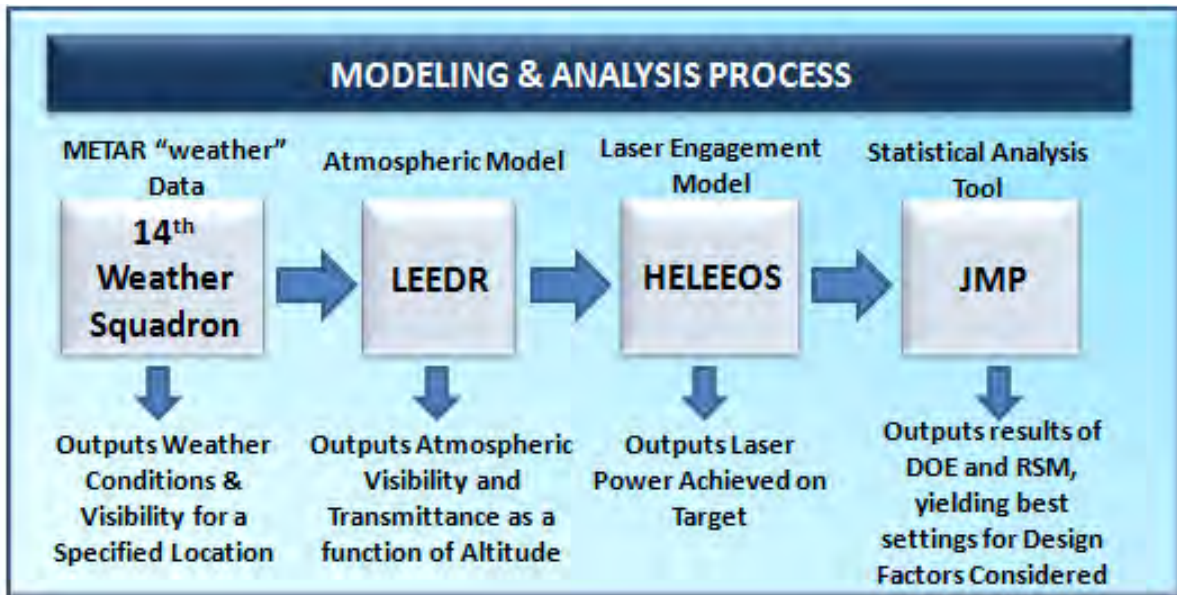


Figure 9: Modeling and Analysis Process

The following sections, 3.41-3.42, provide constant (or baseline) inputs used for HELEEOS and LEEDR to simulate the HEL engagement. Model outputs parameters are also listed for each model. Section 3.5 discusses modifications made to simulate atmospheric variations, including data extracted from the 14th Weather Squadron.

3.41 LEEDR Inputs

Figure 10 displays all inputs required to run LEEDR. The “varied” inputs are considered design factors or nuisance factors. The constant inputs are assumed controlled, and are baseline settings. Nuisance variable inputs are discussed in section 3.5. Design variables are discussed in section 3.62.

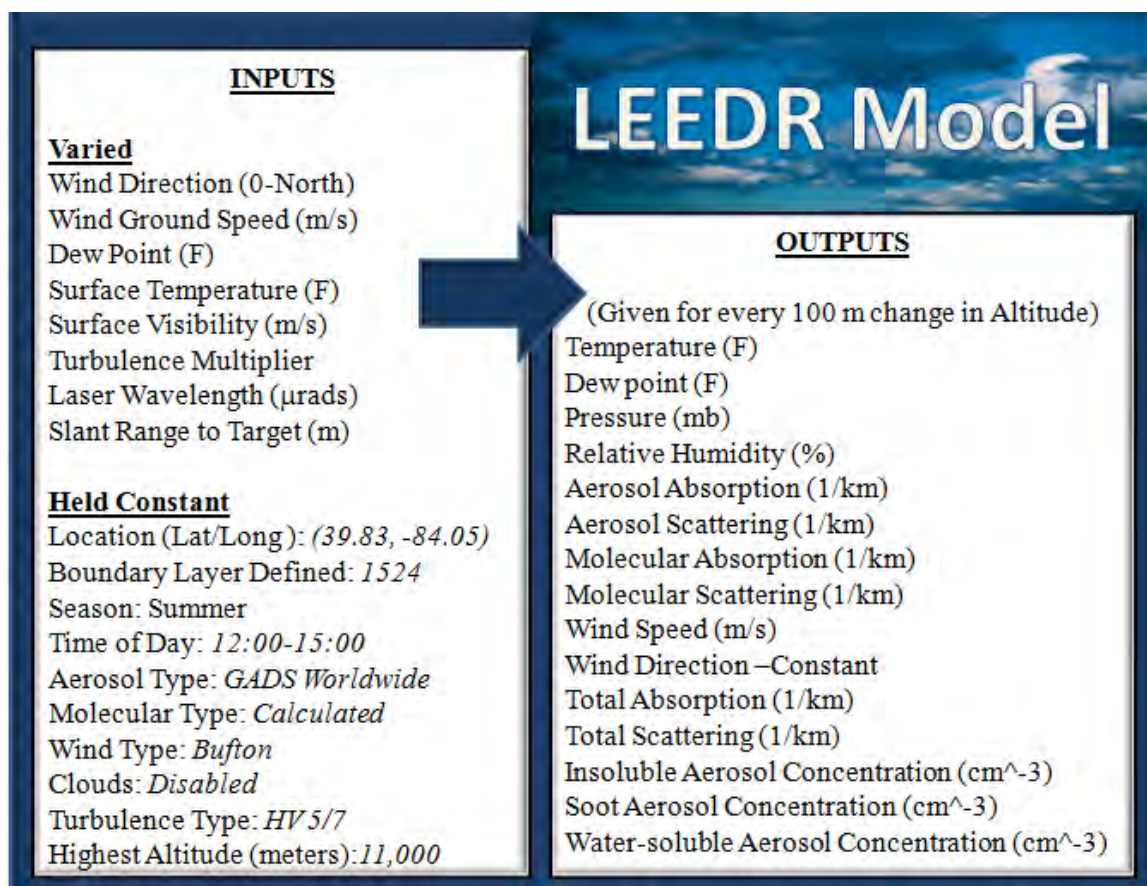


Figure 10: LEEDR Constant Inputs

LEEDR outputs data into an Excel file which is easily imported into HELEEOS. Every design point entered into LEEDR has a distinct atmospheric profile. The random variations induced by the METAR observations have turned LEEDR into a stochastic model which produces a random variable as an output.

3.42 HELEEOS Inputs

Aside from variations introduced by LEEDR's atmospheric profile, HELEEOS also models random variations in platform jitter, discussed in section 3.53. HELEEOS is the last model used, which produces the response data to be analyzed. All held-constant inputs are listed in Figure 11. As mentioned in the baseline development section, many of these inputs have been provided by subject matter experts or borrowed from current Directed Energy programs.

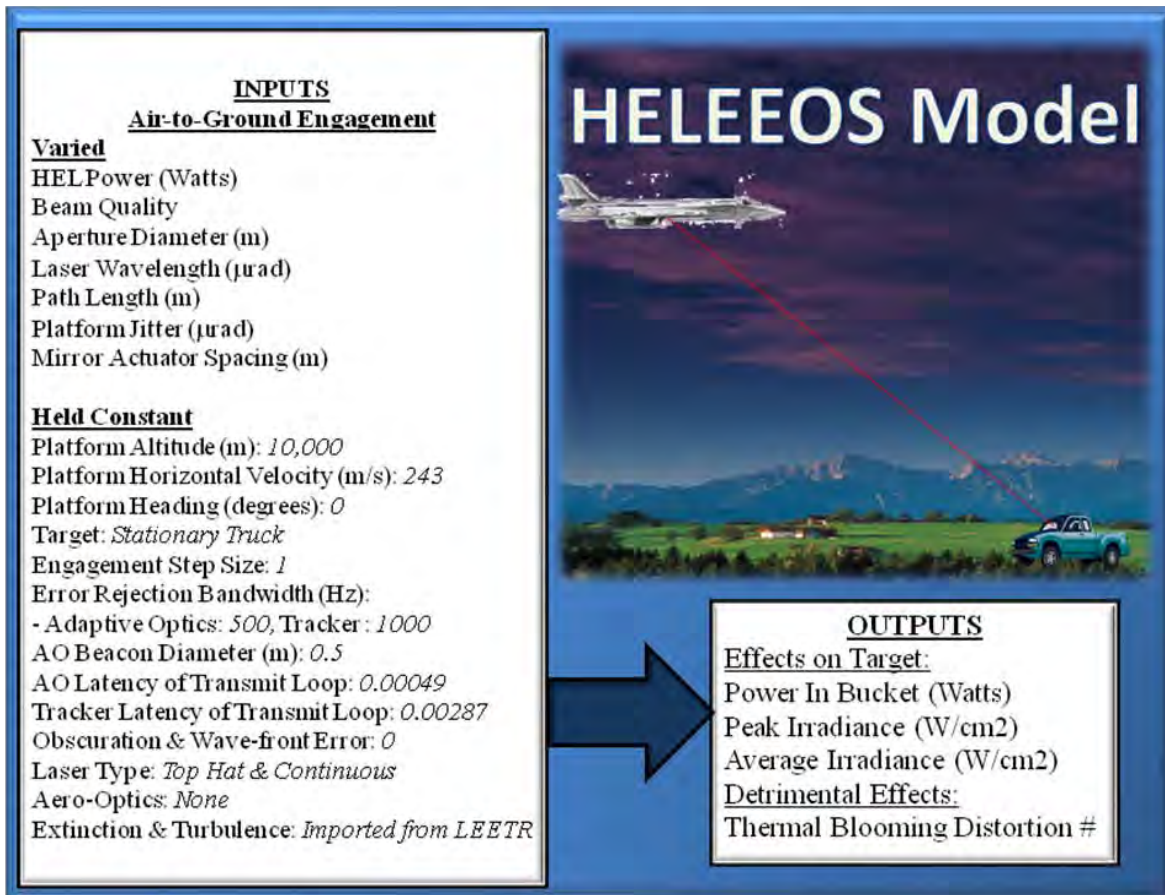


Figure 11: HELEEOS Constant Inputs

3.5 Model Modifications to Simulate Variability of Atmospheric Effects

The process of modeling a stochastic atmosphere for a laser to target engagement was a several step process, due to current limitations of the existing models. Laser propagation codes currently used by the DoD are not stochastic, but rather deterministic. Although the scaling code algorithms are based on probabilities, the outputs themselves are not probabilistic because they are based on atmospheric data over 40 years which has been averaged together, thus diluting the effects of any extreme conditions seen in the tails of the atmospheric probability distribution. To obtain any insights as to how design parameters are influenced by nuisance factors, the nuisance factors must be modeled randomly as they would be found in real life. Modeling variability in the laser engagement came in two forms,

variability associated with the atmosphere, and variability associated with aircraft or “platform” jitter . The following discussion explains the extent of each modification.

3.51 Absorption & Scattering Data from 14th Weather Squadron

The 14th Weather Squadron releases hourly METARs which provide the status of wind (speed & direction), temperature, dew point, visibility at the earth’s surface, and many other conditions for a specified location. METARs are used primarily for aviators wanting to know atmospheric conditions both at the earth’s surface and the sky. For this thesis, the METARs provide data that reflects actual variations found in the atmosphere for a mid-latitude climate. The data types of interest for this study are dew point, pressure, temperature, surface visibility, wind speed, and wind direction. These six METAR outputs are used as inputs into LEEDR. LEEDR takes the weather conditions from the earth-surface, and calculates absorption, scattering, and visibility as a function of altitude. The METARs collected came from the station KFFO, (Dayton, Ohio). Since the summer season was of interest, METAR data was collected for June, July, and August for the last 5 years (2007-present), at 12pm. This interval provided roughly 450 days of Dayton summer at noon, which captures both extreme and average-day weather. Random, independent, and identically distributed samples without replacement were pulled from this distribution, providing a unique atmosphere (or absorption and scattering effect) for each simulation run. Refer to Appendix B for the experimental design with actual atmospheric data married to each design point. These are the “varied” inputs entered into LEEDR.

3.52 Turbulence Random Multiplier

HELEEOS 3.0 models turbulence using averaged data which produces deterministic results. Realistically, turbulence is a variable in the atmosphere, and should be modeled stochastically to better represent a dynamic atmosphere. Turbulence exists in any laser propagation test, and varies from test to test. However, turbulence is not an output of METAR reports. One way to simulate turbulence is to use a standard vertical profile of turbulence values from HELEEOS,

i.e. Huff-Nagel Valley 5/7, and vary its strength based on a turbulence multiplier. To determine a reasonable multiplier, a climatological turbulence profile for a mid-latitude location, (i.e.. Dayton, OH), was used to create a representative distribution. The suggested distribution is a lognormal distribution, with mean 0.22, and variance, 0.7 (Fiorino, 2011). We pulled 324 samples from this distribution, assigning each design point an independent and identically distributed random turbulence multiplier. For each replication, the turbulence multiplier is unique. Refer to Appendix C, Turbulence Multiplier and Jitter Inputs for the actual multipliers entered into HELEEOS.

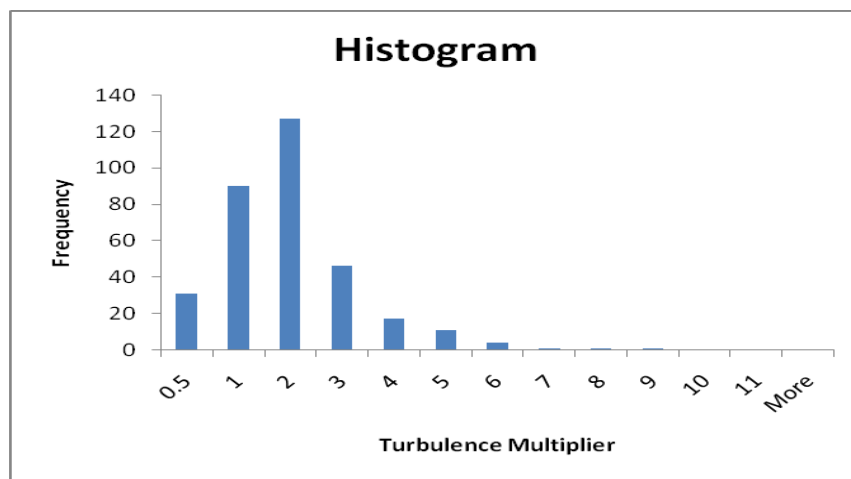


Figure 12: Turbulence Multiplier Distribution

3.53 Platform Jitter Input as a Random Variable

Platform jitter is another nuisance factor which impacts laser beam scattering. There are measures to control some of the platform jitter through vibration tables, however, these methods cannot eliminate the effects of jitter completely. Small amounts of jitter are inevitable, and are thus considered an uncontrolled nuisance factor. In general, the smaller the platform jitter, the less likely we tend to dither the beam on the target at the ground. HELEEOS 3.0 did not have a multiplier to vary this input, thus the input was varied in Excel, then input into HELEEOS. The distribution use to create variable jitter effects was assumed to be a normal distribution, with mean 1 and variance 0.2. A total of 324 samples were

used to create the distribution, assigning each experiment an independent and identically distributed random sample. Although the distribution type is speculative, subject matter experts did give a mean and variance projections for jitter in the year 2022 (Bartell, 2011). This parameter induces variation into the HEL engagement model, and is the only system-related nuisance factor modeled. Each design point tested, and each replication of that design point, has a unique jitter effect.

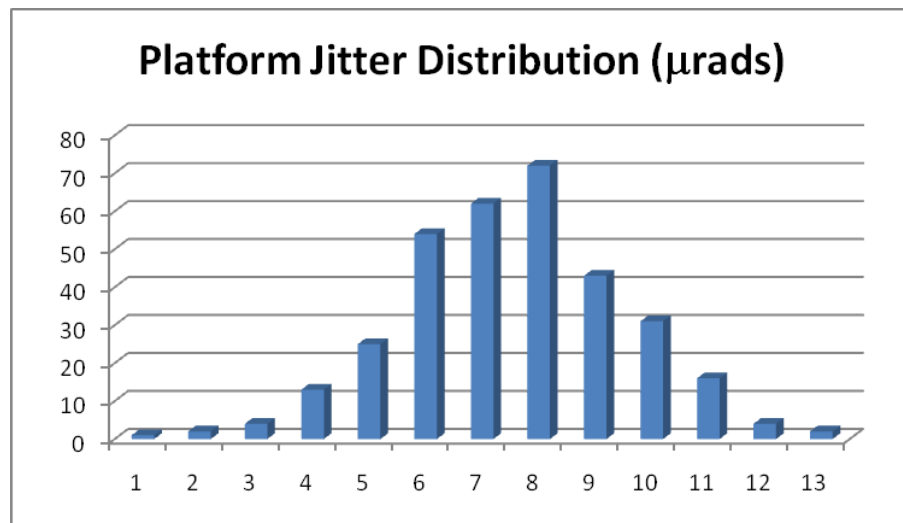


Figure 13: Platform Jitter Distribution

The values used for platform jitter can be seen in Appendix C: Turbulence Multiplier and Jitter Inputs for the actual multipliers entered into HELEEOS

3.6 DOE - Methodology and Experimental Design

This section discusses the experimental design approach. The engagement models an HEL weapon integrated into a B1-B, whose objective is to immobilize a truck from 30,000 ft in the air.

3.61 Defining the Baseline Mission Scenario and Response

The mission scenario modeled for this research is an Air-to-Ground engagement between an airborne HEL weapon system and a stationary target on the ground, a truck. The specifics of this mission scenario come from a current program in the US DoD's Directed Energy Directorate, called the Electric Laser on a Large Aircraft (ELLA). This program is currently integrating a 150 kW laser into the

bomb-bay of Lockheed's B1-B aircraft. There are a variety of Air-to-Air and Air-to-Ground mission vignettes involved in ELLA's test demonstration, both offensive and defensive missions, with targets ranging from stationary, dynamic, and even airborne. For this research, only the Air-to-Ground mission is modeled with a stationary truck as its target. The mission scenario, mid-latitude atmosphere type, aircraft type, flight altitude, engagement slant ranges, aircraft heading, and aircraft speed parameters were all provided by the ELLA analysis team, and used to establish the baseline results. The actual values for these parameters are listed in sections 3.41 LEEDR Inputs and 3.42 HELEEOS Inputs.

A mid-latitude climate was selected for the Air-to-Ground engagement scenario modeled. This selection is based upon subject matter expert input regarding countries of interest to the US Air Force having mid-latitude climates. Dayton, Ohio, was selected as the location for the scenario modeled in this thesis due to its mid-latitude location. As seen in Figure 14, climates tend to be consistent relative to their distance from the equator.

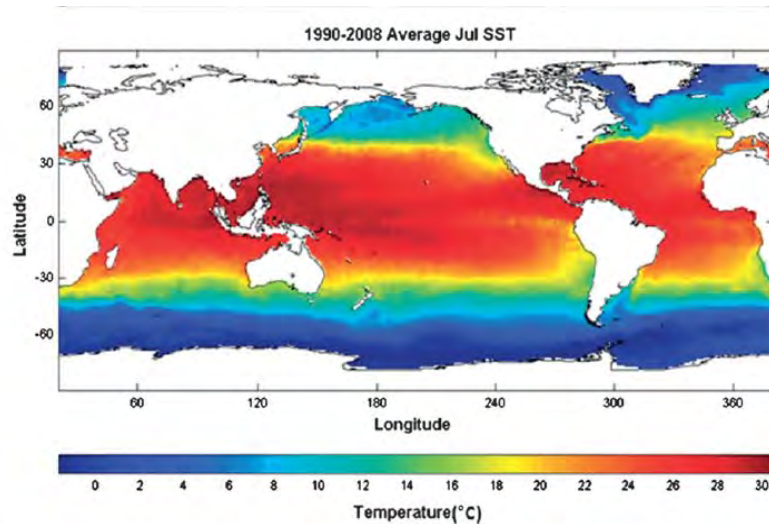


Figure 14: Monthly mean SST calculated from the gridded GTSP data from 1990 to 2008 during (top) January and (bottom) July (Fiorino, 2008)

The response variables chosen for this research were Power in Bucket (PIB) (watts) and Average Irradiance (watts/cm^2) within a 10 cm diameter bucket. PIB and Average Irradiance provide the amount of energy per cm^2 deposited on the target.

While these parameters alone will not reflect the achieved damage to target, however, they do provide a basis to compare the performance between design points.

3.62 Design Factor, Level, and Range Selection


Design Factors: For an Air-to-Ground laser weapon engagement there are numerous controllable factors. These factors relate mostly to HEL characteristics (power level, wavelength), optics specifications, as well as engagement geometry (aircraft flight altitude and slant range). There are a variety of ways to choose factors to control in a test or experiment. Using author judgment, based on four years of modeling laser weapon system engagements for the Directed Energy Directorate, in which numerous sensitivities and trade-space assessments were completed, the design factors selected include laser output power, aperture size, beam quality, wavelength, and slant range (propagation path, or range from aircraft to target).

Levels and Ranges: Each design factor requires a range and levels to be tested (i.e. Power level from range 100kw-400kw, test at 3 levels, 100kw, 200kw, and 400kw). Ideally, the rule of thumb in selecting a range is to capture three standard deviations (99.73%) of variation in the response. This rule is based on the concept that you want to capture a broad enough range to detect a difference between levels, yet not so broad that only the extreme cases are captured.

Due to physical weight and volume limitations of what a B1-B aircraft can support for a laser weapon system, the range for HEL power was kept between 100kW and 400kW. As for wavelength, many sensitivity studies have been performed to narrow in on which are the best to propagate through atmosphere, and those that are near 1 μm include: 1.03 μm , 1.045 μm , and 1.064 μm (Fiorino, 2011). The aperture size is also limited by the weight and volume capacity of the beam director on the B1-B aircraft; apertures exceeding 70 cm (diameter) are not worth the cost in weight and volume, and apertures less than 25 cm are not large enough to achieve desired performance results. The slant ranges selected for this research were

taken from the ELLA program test demonstration requirements. Table 1 displays the design factors and the levels and ranges in which they are varied in the models.

Table 1: Design Factors - Levels and Range Varied

DESIGN FACTORS		Levels	Ranges			
A	Beam Quality	3	1	1.5	2	
B	Aperture Diameter (cm)	3	30	50	70	
C	Wavelength (μm)	3	1.0642	1.045	1.03	
D	Slant Range (km)	3	11	17	25	
E	Power (kW)	4	100	150	250	400

3.63 Experimental Design Selection

The design factor levels and ranges shown in Table 1 would require a full, mixed factorial design with of 3 level^(4 factor) x 4 level^(1 factor) = $(3^4)(4) = (81)(4) = 324$ possible combinations, or design points. Since variability is in the HEL engagement model, replications are needed to help provide a better estimate of the pure error in the model, as well as provide a better estimate of average response. Given three replications at each design point yields 324×3 replications = 972 total observations. A fractional design provides the design reduction needed while still allowing for estimates of the main effects. This is done by aliasing in the half fraction factorial design eliminating the ability to estimate higher order interactions. Implementing this design yields $(3^3)(4^1) = 108$ design points. With three replications, this yields a total of 324 total observations. The final experimental design is provided in Appendix A: Experimental Design.

3.7 Summary

This thesis addresses two methodological issues new to HEL modeling. First, it improves predictive capabilities in modeling HEL engagements by incorporating atmospheric variations. Second, by applying DOE, parameters are varied in factorial designs, in random order, and with replications, which provide a statistical basis to objectively compare design points and make valid conclusions. These approaches

allow insights into the portion of performance attributed to design factors, and what portion is attributed to nuisance factors.

IV. Results and Analysis of Key Design Factors

4.1 Experienced-Based Expectations of the Research


The design factors selected for the experimental design were selected based on prior knowledge that they are key performance parameters which drive HEL performance. Although these factors have been modeled and studied extensively, they typically have been varied in a one factor at a time manner, eliminating insights to relationships and interactions between parameters. Most HEL modeling approaches also lack stochastic modeling of atmospheric conditions. This chapter demonstrates the advantages using an experimental design to analyze interactions and quadratic effects, as well as advantages to incorporating noise to differentiate between cause and effect relationships.

For the analysis, it was assumed the best HEL system design for the Air-to-Ground engagement modeled would be an HEL laser with 400kW power, beam quality of 1, 70 cm aperture, and 11 km slant range to target. These scenario parameters were based on the idea that more power yields a greater intensity, beam quality of 1 yields the tightest beam possible, a 70 cm aperture will magnify the intensity greater than smaller sizes, and 11 km is a reasonably close engagement range, enabling a shorter distance for the beam to propagate through the atmosphere. The following sections address research findings and provide insights into best parameter settings suggested by the experimental data.

4.2 Experimental Design

The experimental design used for this research is a factorial design composed of five design factors: beam quality, aperture size, laser wavelength, slant range, and HEL power. Each parameter is varied at three levels, with the exception of HEL power, varied at four levels shown in Table 2.

Table 2: Design Factors - Levels and Range Varied

DESIGN FACTORS		Levels	Ranges			
A	Beam Quality	3	1	1.5	2	
B	Aperture Diameter (cm)	3	30	50	70	
C	Wavelength (μm)	3	1.0642	1.045	1.03	
D	Slant Range (km)	3	11	17	25	
E	Power (kW)	4	100	150	250	
					400	

HELEEOS is used to generate power in bucket (PIB) intensities on target, based on the design settings. Nuisance factors, such as absorption, scattering, turbulence, and platform jitter are also modeled. Absorption and scattering effects are modeled using LEEDR, which takes real METAR observations from a geographic location (Dayton, OH), interpolates upper air conditions. These conditions are used to calculate absorption and scattering effects by percent transmittance for the modeled laser. Turbulence was calculated within HELEEOS, and multiplied by a random multiplier from a lognormal distribution ($\mu = 0.22$, $\sigma=0.7$) to replicate the stochastic nature of turbulence. Jitter, a platform vibration interference, was modeled as a random variable as well. Platform jitter inputs were pulled from a normal distribution ($\mu=1$, $\sigma=0.2$). The distributions for turbulence and jitter were provided by subject matter experts in the Directed Energy modeling community (Fiorino and Bartell, 2011).

The experimental design is located in Appendix B and C. Each design point has a unique set of nuisance effects, making the response a random variable. Since these variations can dilute the traceability of an effect on a response, each design point is replicated three times.

Four response variables are produced by HELEEOS and collected for each design point tested. These response variables are PIB (in Watts), averaged irradiance (in Watts/cm²), atmospheric transmittance (in %), and a thermal blooming distortion number. PIB is used for statistical analysis and to interpret effects of interest. The objective is to isolate the largest sources of variation caused to the response

variables, and identify the dependencies that exist. Sources of variation are due to main effects, interactions between two or more effects, non-linear effects, and error.

4.21 Key Aspects to a Good Model

Statistical tools are very helpful, however they are based on statistical principles that must be valid in order to use the tools to make statistical conclusions.

Model Adequacy - Model adequacy is achieved by the satisfaction of three statistical assumptions: residuals (difference between actual and predicted values) are independent, with zero mean, constant variance σ , and are normally distributed.

Model Fit – An empirical model is a linear model representation of a system or process. “Lack-of-fit” is the calculation which reflects how well an empirical model fits data. Lack-of-fit compares estimates of error to residual error to determine whether significant effects are left out of the model. Reducing lack of fit generally involves adding effects to the model, such as interactions or nonlinear terms, or linearizing the response using some transformation.

Model Significance –Statistical significance for an effect is based upon the units of variations explained by the effect in comparison to error. Mean square captures units of explained variation, while as a function of the dimensions of design space considered. The ratio of mean square model to mean square error is called an F-ratio and follows an F-distribution when the model effect is zero. As the F-ratio becomes large, the probability of the variation due to error decreases and probability of the variation due to the model, or model components, increases. These probabilities are called p-values.

If assumptions of normality of residuals and constant variance are not satisfied for a given model, then statistical inferences are tenuous. Often in the real world analysis, non-linear nuisance factors interfere with getting “clean” data, making it hard to fit an empirical model and achieve model adequacy. In cases such as these, data can still be analyzed, and although statistical inferences cannot be made, practical inferences can be made. Practical inferences are typically conservative, as to reflect less confidence about the data. An assumption can be

made regarding F-ratios, and what level will be deemed significant because the F-ratio is really the ratio of variance explained by the model component to model error. It is appropriate to assume a large F-ratio, for instance three times the magnitude of the error, means changes in our response are due to something other than error. Thus, an F-ratio of 3 or higher is deemed to have practical significance in driving system performance when we cannot make firm statistical statements.

4.22 Full Model Results

The full empirical model for the Air-to-Ground engagement captures all possible combinations of design factors, to include two-way interaction effects, non-linear effects, and main effects. This model design factors, or regressors, are listed in the “source” column in Table 3. This empirical model is based on PIB outputs from HELEEOS. Actual PIB values and other response variables are located in Appendix D. All variations to the response not explained by the effects in the model are considered pure error.

Table 3: Parameter Estimates

Source	Estimated Coefficient	Standard Error	Type Effect
Intercept	434390.24	78562.05	-
Beam Quality	-10148.42	2607.779	Main
Aperture	888.33868	62.99037	
Wavelength	-307392.9	75234.95	
Slant Range	-6737.812	189.2597	
Power	200.39097	11.35191	
Beam Quality*Beam Quality	3668.9063	8755.601	Non-Linear
Beam Quality*Aperture	417.03347	162.181	Interaction
Aperture *Aperture	-1.470799	5.521688	Non-Linear
Beam Quality*Wavelength	138639.7	188452.1	Interaction
Aperture *Wavelength	-2798.504	4631.632	Interaction
Wavelength *Wavelength	-33803202	7652839	Non-Linear
Beam Quality*Slant Range	1298.4399	474.4251	Interaction
Aperture *Slant Range	-18.51438	11.27882	Interaction
Wavelength *Slant Range	-7357.662	13082.3	Interaction
Slant Range *Slant Range	360.14319	45.70288	Non-Linear
Beam Quality*Power	35.773023	24.13629	Interaction
Aperture *Power	3.3650923	0.571072	Interaction
Wavelength *Power	-1975.067	658.7468	Interaction
Slant Range *Power	-22.87221	1.70417	Interaction
Power *Power	-0.487425	0.110281	Non-Linear

This full model was not found adequate in the statistical assumptions. Residuals are fit to a normal distribution. Figure 15 shows a relatively decent fit, with the exception of the tails. The fit is evaluated by a Shapiro-Wilk “goodness-of-fit” test, and generates a p-value of <.0001, which rejects a null hypothesis that residuals are normally distributed. Thus, the full empirical model does not satisfy the first assumption of normality of residuals.

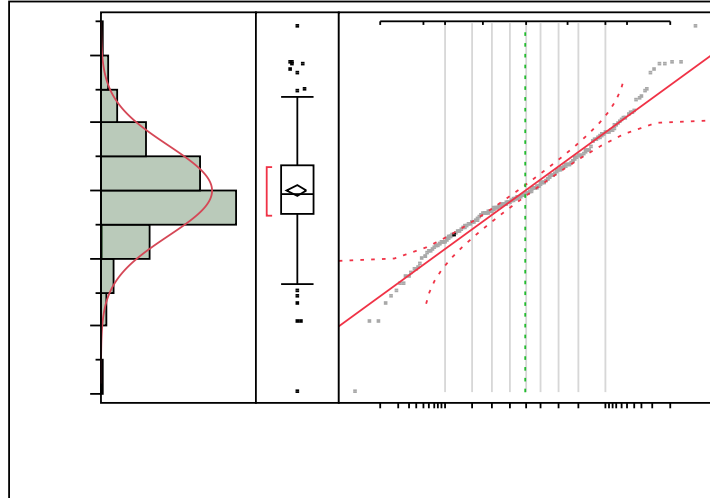


Figure 15: Residuals Evaluated for Fit to Normal Distribution

Figure 16 plots residuals versus the predicted response. The distinct cone pattern indicates a non-constant variance.

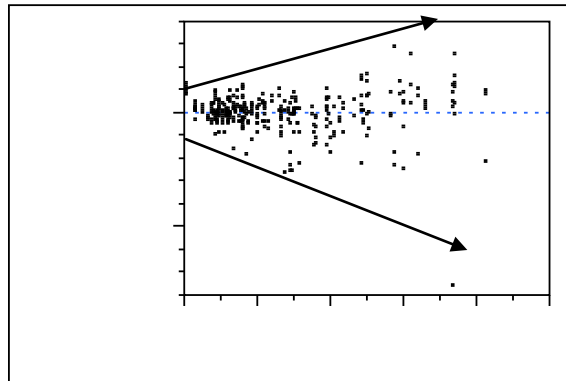


Figure 16: Residual by Predicted Plot

Eight transformations were examined: Box Cox, log, square root, square, reciprocal, exponential, Arrhenius, and Arrhenius-inverse. No transformations rectified the residual issues. Non-significant terms are also removed from the model, however the reduced models still failed to satisfy normality of residuals and a constant variance.

Since model adequacy fails, practical inferences are made. The analysis of variance, in Table 4, shows the mean square of the model versus mean square of the error. A model F-ratio of 113.8 ($MS_{\text{model}}/MS_{\text{error}}$) is large enough to imply it has practical significance. The model explains 113 times more of the response

variability than does error. With this much variation explained by the model, there are important terms in the model.

Table 4: Analysis of Variance

Source	Degrees of Freedom	Sum of Squares	Mean Square	F Ratio	Prob > F
Model	20	7.5381e+11	3.769e+10	113.7988	<.0001*
Error	303	1.0035e+11	331203848		
Total	323	8.5417e+11			

Table 5 lists the effects within the full model, along with the units of variation of PIB they explain. Each effect element of the model consists of one degree of freedom. Given a rule of thumb that a F-ratio higher than 3 has practical significance, thirteen of the twenty factors (bolded in table) satisfy this condition (these factors also have small p-values indicating statistical signature if model adequacy checks passed). Effects of most interest are: slant range, HEL power, and Aperture size. An interesting observation are the non-linear relationships with PIB, such as power and slant range, which also explain a fairly large portion of PIB variance.

Table 5: Parameter Estimates and Contribution to Power in Bucket (PIB)

Source	Estimated Coefficient	Standard Error	Sum of Squares	F Ratio	Prob > F
Intercept	434390.24	78562.05			
Beam Quality	-10148.42	2607.779	5002643875	15.1445	0.0001*
Aperture	888.33868	62.99037	6.5698e+10	198.8881	<.0001*
Wavelength	-307392.9	75234.95	5514326286	16.6935	<.0001*
Slant Range	-6737.812	189.2597	4.1866e+11	1267.423	<.0001*
Power	200.39097	11.35191	1.0293e+11	311.6151	<.0001*
Beam Quality*Beam Quality	3668.9063	8755.601	58002323.6	0.1756	0.6755
Beam Quality*Aperture	417.03347	162.181	2184167058	6.6121	0.0106*
Aperture *Aperture	-1.470799	5.521688	23437258.3	0.0710	0.7901
Beam Quality*Wavelength	138639.7	188452.1	178779336	0.5412	0.4625
Aperture *Wavelength	-2798.504	4631.632	120594590	0.3651	0.5462
Wavelength *Wavelength	-33803202	7652839	6444876122	19.5106	<.0001*
Beam Quality*Slant Range	1298.4399	474.4251	2474301397	7.4905	0.0066*
Aperture *Slant Range	-18.51438	11.27882	890092915	2.6946	0.1017
Wavelength *Slant Range	-7357.662	13082.3	104485318	0.3163	0.5743
Slant Range *Slant Range	360.14319	45.70288	2.0512e+10	62.0959	<.0001*
Beam Quality*Power	35.773023	24.13629	725628346	2.1967	0.1393
Aperture *Power	3.3650923	0.571072	1.147e+10	34.7226	<.0001*
Wavelength *Power	-1975.067	658.7468	2969412978	8.9893	0.0029*
Slant Range *Power	22.87221	1.70417	5.9502e+10	180.1317	<.0001*
Power *Power	0.487425	0.110281	6452926019	19.5350	<.0001*

The full model yields an $R^2 = 0.88$, which means roughly 88% of the variance within the response is explained by the empirical model, and 12% explained by error, nuisance factors, or insignificant factors grouped in the error term. Table 6 indicates some lack of fit of the model to the data; however with the rule of thumb of F-ratio being larger than 3, it does not have practical significance. The F-ratio for lack of fit is quite small. The large degrees of freedom for pure error make the F-test somewhat sensitive. The small F-ratio leads to accepting the full model, discounting the lack of fit. There might be non-linear effects in the residual error due to nuisance factors such as thermal blooming; this is examined later.

Table 6: Lack of Fit

Source	Degrees Freedom	Sum of Squares	Mean Square	F Ratio	Prob > F
Lack of Fit	75	3.4595e+10	461267121	1.599	0.0045*
Pure Error	228	6.576e+10	288419876		
Total Error	303	1.0035e+11			

4.23 Full Model With Poor Visibility Conditions Removed

Influential points are known to skew data distributions, and are typically located at the tails of a normal fit (such as the s shaped series of points deviating from the normal fit in Figure 15). Suspect points were evaluated and traced back to the model inputs of HELEEOS and LEEDR. The cause of the influence was successfully traced back to poor atmospheric visibility conditions of less than 16 statute miles. These influential points were removed, and the model is re-evaluated. The model listed in Table 7 captures the full model, with extreme visibility conditions removed.

Table 7: Full Model without Poor Visibility - Parameter Estimates

Source	Estimated Coefficient	Standard Error
Intercept	456883.09	52895.07
Beam Quality	-9295.873	1751.37
Aperture	857.69105	42.34575
Wavelength	-326801.6	50537.65
Slant Range	-6837.294	128.9379
Power	213.26772	8.121139
(Beam Quality-1.49)*(Beam Quality-1.49)	1205.0169	5983.174
(Beam Quality-1.49)*(Aperture-50.28)	416.0535	106.5034
(Aperture-50.28)*(Aperture-50.28)	-12.09237	3.718925
(Beam Quality-1.49)*(Wavelength-1.05)	109334.92	127652.4
(Aperture-50.28)*(Wavelength-1.05)	-5076.473	3105.392
(Wavelength-1.05)*(Wavelength-1.05)	-29715285	5101571
(Beam Quality-1.49)*(Slant Range-17.73)	1251.8943	313.1371
(Aperture-50.28)*(Slant Range-17.73)	-18.27814	7.694775
(Wavelength-1.05)*(Slant Range-17.73)	342.44749	8869.147
(Slant Range-17.73)*(Slant Range-17.73)	377.97088	30.59005
(Beam Quality-1.49)*(Power-220.24)	47.225295	16.87139
(Aperture-50.28)*(Power-220.24)	3.3748452	0.388284
(Wavelength-1.05)*(Power-220.24)	-2131.118	456.1259
(Slant Range-17.73)*(Power-220.24)	-24.38194	1.200517
(Power-220.24)*(Power-220.24)	-0.390279	0.074323

Figure 17 shows that the residuals from the updated model do fit a normal distribution. This model passes a Shapiro-Wilk goodness of fit test with a p-value of 0.18, thus residuals are normally distributed.

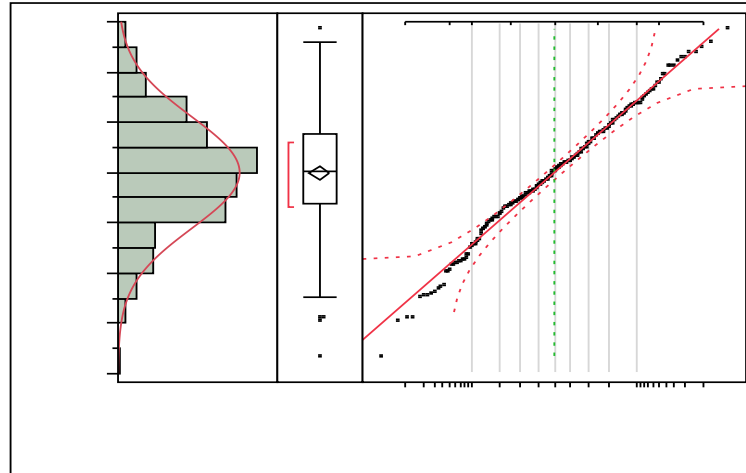


Figure 17: Normal Distribution of Residuals (with Poor Visibility Conditions Removed)

Figure 18 shows the model residuals versus the predicted response. The residuals have a slight pattern, which can indicate a non-constant variance. Transformations are examined, and a square root transformation of the response removes this pattern. Figure 19 shows the residual versus predicted response after the transformation.

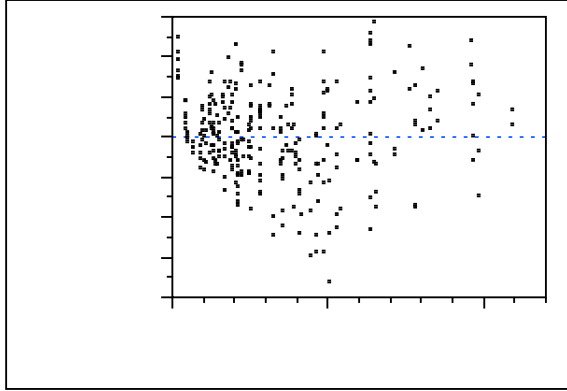


Figure 18: Residual by Predicted

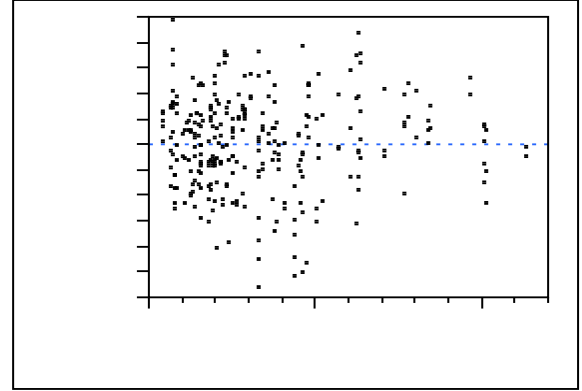


Figure 19: Residual by Predicted (with Square Root Transform on Response)

This statistically adequate model has an R^2 value of 0.96. The model has a significant lack of fit with a F-ratio of 3.4, however, leverage plots of effects versus the response were examined, and all appeared fairly linear, thus the lack of fit is likely due to non-linear atmospheric effects captured in the error term or sensitivity due to the high number of degrees of freedom for pure error. Model details are presented in next section in comparison with our initial model.

4.24 Side-by-Side Comparison of Models

Table 8 compares both the full model with all points and the full model with the poor atmospheric visibility points removed. Practical significance is used to make inferences in the full model (with all observations), and statistical significance is used to interpret the full model with selected points removed (use of a p-value). Nearly all terms in the second model are statistically significant at the 0.05 level (asteriked in Table 8). Significant terms are in bold. In comparison, both models agree that slant range, power, aperture, and interactions between slant range and other parameters explain the majority of variation over other parameters in the model. However, F-ratios for aperture² and wavelength differ. The difference in wavelength significance may be due to the idea that if poor visibility conditions exist, it does not matter which type of wavelength propagates, all are wiped out. Whereas if good weather conditions exist, wavelength will have an influence on HEL propagation.

Table 8: Model Comparisons - With and Without Poor Visibility Conditions

	Full Model		Full Model w/Points Removed		
Source	Sum of Squares	F Ratio	Sum of Squares	F Ratio	P-Value
Slant Range	4.19E+11	1267.423	1317971.8	3642.304	<.0001*
Power	1.03E+11	311.6151	282437.6	780.5353	<.0001*
Aperture	6.57E+10	198.8881	224666.1	620.8799	<.0001*
Slant Range*Power	5.95E+10	180.1317	81830.6	226.1444	<.0001*
Slant Range*Slant Range	2.05E+10	62.0959	25217.5	69.6901	<.0001*
Aperture*Power	1.15E+10	34.7226	13719.8	37.9156	<.0001*
Power*Power	6.453E+09	19.535	17920.8	49.5253	<.0001*
Wavelength*Wavelength	6.445E+09	19.5106	14307.3	39.5393	<.0001*
Wavelength	5.514E+09	16.6935	24561.1	67.8761	<.0001*
Beam Quality	5.003E+09	15.1445	16995.4	46.968	<.0001*
Wavelength*Power	2.969E+09	8.9893	5510.7	15.2292	<0.0001*
Beam Quality*Slant Range	2.474E+09	7.4905	2658.5	7.3468	0.0072*
Beam Quality*Aperture	2.184E+09	6.6121	6361.8	17.5813	<.0001*
Aperture*Slant Range	890092915	2.6946	3528.3	9.7506	0.0020*
Beam Quality*Power	725628346	2.1967	3288.4	9.0876	0.0028*
Beam Quality*Wavelength	178779336	0.5412	240.9	0.6657	0.4153
Aperture*Wavelength	120594590	0.3651	318.6	0.8805	0.3489
Wavelength*Slant Range	104485318	0.3163	1349.1	3.7283	0.0546
Beam Quality*Beam Quality	58002324	0.1756	352.2	0.9735	0.3247
Aperture*Aperture	23437258	0.071	6236.1	17.234	<.0001*

Although it is important to identify and understand influential points and how they alter results, they cannot be removed from the model without justification. Even though it is impractical for lasers to be tested on very poor visibility days, the initial model with the influential points is used to conduct analysis, keeping in mind statistical inferences may be suspect, but practical significance can be applied.

Had a deterministic model been used to model this Air-to-Ground engagement, there would be no variation in the response. A stochastic model, that involves nuisance factors, provides a basis to determine if an effect is meaningful to the

response it generates. A stochastic model also reflects which effects are likely obscured in a live test. Design of experiments in modeling and simulation can be used to make projections for tests, or more effectively and efficiently design tests to estimate factors of interest.

4.25 Response Surface of Full Model

Varying one factor at a time during a test allows us to estimate main effects. Varying multiple factors at a time allows us to estimate interactions. Response surface methodology allows us to evaluate any non-linear effects that may exist within a model. We can also generate graphical plots depicting factor influence on responses of interest. While limited to just two factors at a time, the collective examination of the surfaces reveals tremendous insight into the multi-dimensional surface that describes how the response varies as a function of factor levels.

In the full model, the non-linear terms believed to have practical significance, (due to a F-ratio >3), are slant range², wavelength², and power². The interactions terms believed to have practical significance are slant range*power, aperture size*power, wavelength*power, beam quality*slant range, and beam quality*aperture size. The response surface of each of these non-linear and interaction terms are evaluated. Beam Quality is unit-less, aperture size is in cm² diameter, HEL power is in kilowatts, slant range in km, wavelength in μm , and PIB in watts. Figures 20-22 show the non-linear relationship between individual parameters (slant range, wavelength and power) and their response, PIB. These parameters are practically significant as main effects, and as non-linear effects.

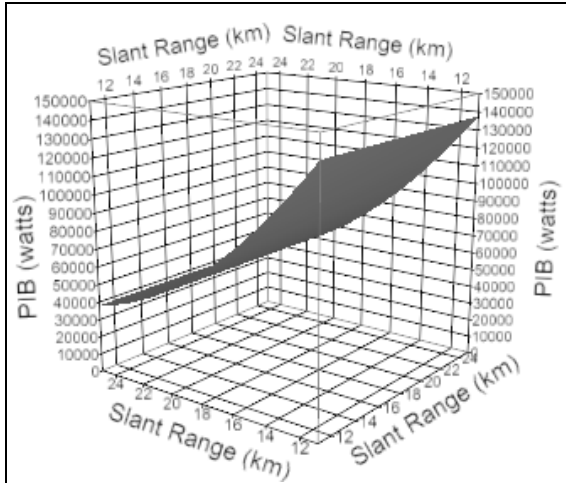


Figure 20: Response Surface of Slant Range² vs. PIB

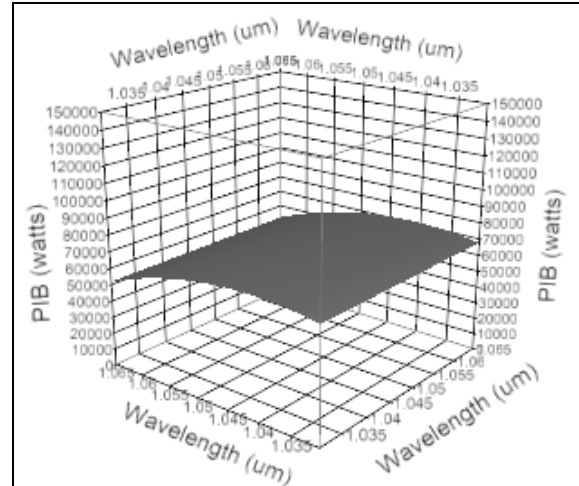


Figure 21: Response Surface of Wavelength² vs. PIB

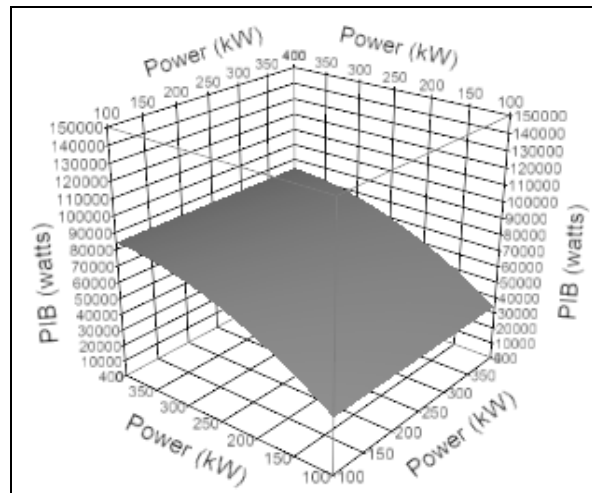


Figure 22: Response Surface of Power² vs. PIB

Figures 23-27 show all response surface interactions believed to have practical significance in the model. The non-linearity is likely to be caused by the way each parameter is effected by thermal blooming, a non-linear nuisance factor. Figure 4 shows an interaction between power and slant range having a non-linear effect on PIB.

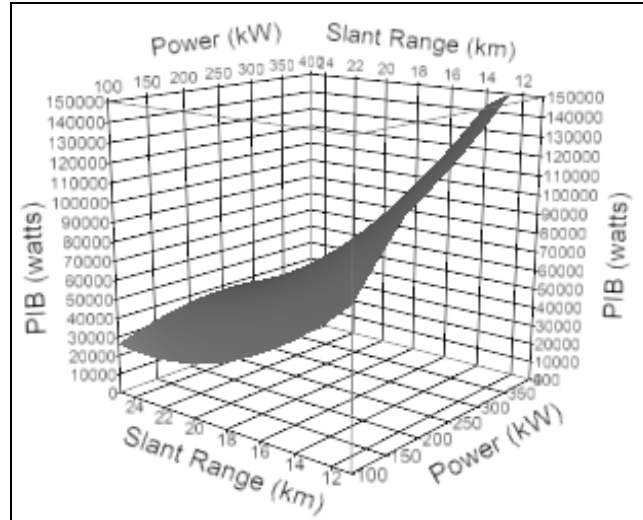


Figure 23: Response Surface of Power*Slant Range vs. PIB

Figure 24 shows the non-linear relationship between HEL power and aperture size. The higher the HEL power level, the hotter the atmosphere becomes as the beam propagates through it, thus increasing atmospheric absorption and thermal blooming. The bigger the aperture, the more focused the beam is, creating more intensity in a tighter beam. Given the correlation between these two parameters on beam intensity during propagation, the relationship makes sense, as well as the non-linear influence of thermal blooming.

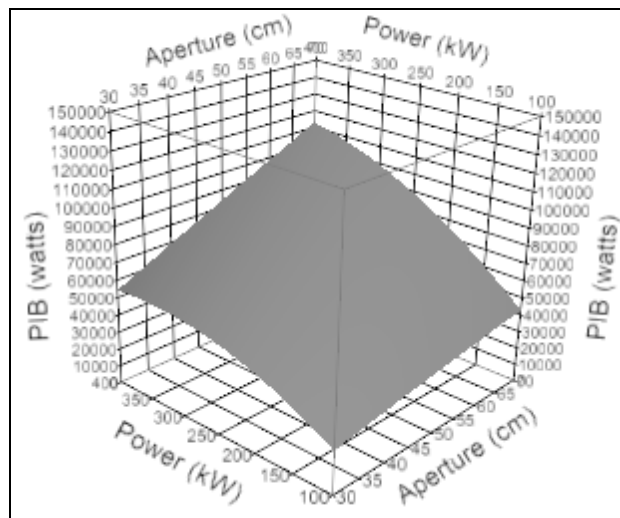


Figure 24: Response Surface of Power*Aperture vs. PIB

Figure 25 shows the response surface of power and wavelength versus PIB. Wavelength does influence the speed in which a beam propagates through an atmospheric medium, and larger wavelengths tend to suffer greater beam loss due to absorption. Power on the other hand has a cost-benefit relationship with PIB, where the higher the power the more intensity on target. Higher power also increases thermal blooming, which causes loss to PIB.

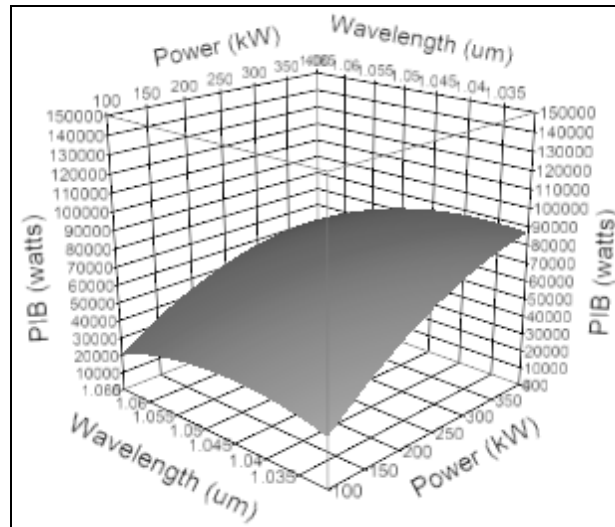


Figure 25: Response Surface of Power*Wavelength vs. PIB

Figure 26 shows the interaction between slant range and beam quality as it effects PIB. Since these parameters are not highly dependent on thermal blooming, there is very little curvature seen.

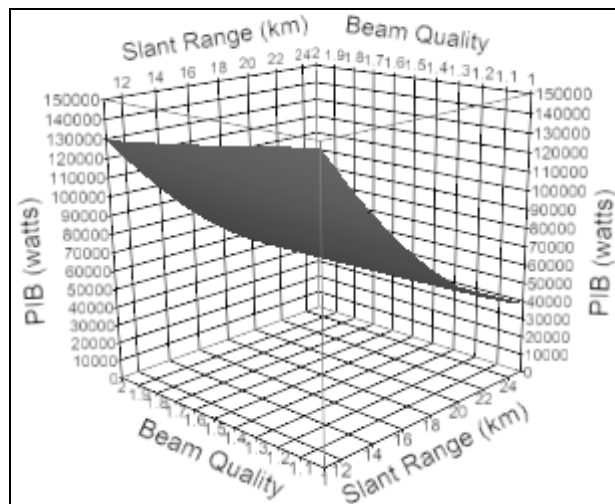


Figure 26: Response Surface of Slant Range*Beam Quality vs. PIB

Figure 27 shows the response surface between aperture size and beam quality vs. PIB. Apertures cause a more focused beam, whereas beam quality relates to how spread out the beam is; tighter is better. The aperture focuses a beam on target, and beam quality can have the effect of defocusing a beam, which would be the same effect as making the aperture smaller. These two parameters play against one another during trade studies.

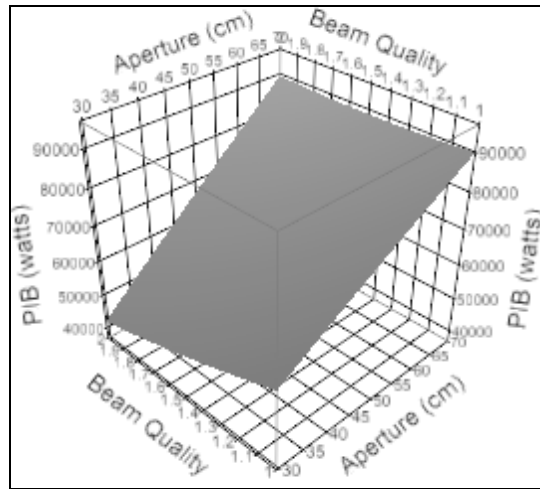


Figure 27: Response Surface of Aperture Size*Beam Quality vs. PIB





















The cost-benefit relationships between parameters is clearly complex, and interpretations are hard to do without extensive knowledge of atmospheric and HEL physics. Had these interactions and non-linear effects not been included in the model, they would have been mistakenly been captured in error thus obscuring other effects. Given these non-linear effects play a significant role in HEL modeling, analysis conducted without incorporating their effect may be misleading.

4.26 A look at Thermal Blooming

One of the response variables collected from HELEEOS was a thermal blooming distortion. An empirical model is examined with the full model (all main, interaction, and non-linear effects), but with thermal blooming as a response. Although the residuals fail both the assumption of normality and constant variance, an F-ratio practical significance can be used to interpret the model. Table 9 shows

that power and aperture size have the greatest effect on thermal blooming, based on F-ratios far greater than 3.

Table 9: Parameter Effects in Relation to Thermal Blooming

Term	Estimate	Std Error	F Ratio	Contribution to Variation in Response	Prob> t
Power	0.965199	0.069373	193.57		<.0001*
Aperture	2.712575	0.38494	49.66		<.0001*
Slant Range	7.064078	1.156584	37.3		<.0001*
(Aperture-50)*(Power-225)	0.014917	0.00349	18.27		<.0001*
(Wavelength-1.05)*(Wavelength-1.05)	182943.8	46767.24	15.30		0.0001*
(Aperture-50)*(Slant Range-17.7)	0.195441	0.068926	8.04		0.0049*
(Slant Range-17.7)*(Power-225)	0.027275	0.010414	6.86		0.0093*
(Wavelength-1.05)*(Slant Range-17.7)	200.0598	79.94723	6.26		0.0129*
Wavelength	856.6778	459.768	3.47		0.0634
(Wavelength-1.05)*(Power-225)	7.255168	4.025665	3.24		0.0725
(Beam Quality-1.5)*(Power (kW)-225)	0.231795	0.147499	2.47		0.1171
(Beam Quality-1.5)*(Slant Range-17.7)	-3.79111	2.899257	1.71		0.1920
(Slant Range-17.7)*(Slant Range-17.7)	-0.276393	0.279295	0.98		0.3232
(Aperture-50)*(Wavelength-1.0464)	-27.33041	28.30435	0.93		0.3350
(Aperture-50)*(Aperture-50)	-0.02869	0.033744	0.72		0.3959
(Beam Quality-1.5)*(Wavelength-1.05)	773.8866	1151.649	0.45		0.5021
(Power-225)*(Power-225)	0.000359	0.000674	0.28		0.5943
(Beam Quality-1.5)*(Aperture-50)	0.462790	0.991104	0.21		0.6409
(Beam Quality-1.5)*(Beam Quality-1.5)	14.88194	53.50633	0.07		0.7811
Beam Quality	-0.160628	15.93639	0.0001		0.9920

4.3 Optimal System Design & Test Design for the Specified Mission Scenario

The highly non-linear response surface was found to have a saddle point structure. Thus, using the canonical analysis component of RSM did not yield an optimal design setting within the factor space considered. A nonlinear constrained optimization problem was solved using LINGO. The objective is to maximize PIB by finding the combination of settings that yield greatest intensity on target. The following constraints are use to bound the solution within the design space.

- 1) $1 \leq \text{Beam Quality} \leq 2$
- 2) $30 \text{ cm} \leq \text{Aperture Size} \leq 70 \text{ cm}$
- 3) $1.03 \mu\text{m} \leq \text{Wavelength} \leq 1.0642 \mu\text{m}$
- 4) $11 \text{ km} \leq \text{Slant Range} \leq 25 \text{ km}$
- 5) $100 \text{ kW} \leq \text{HEL Power} \leq 400 \text{ kW}$

Table 10 shows the solution output from LINGO, achieving a maximum PIB of 171,840.9 Watts. Note, this may not be a unique optimal solution.

Table 10: Solution to Design

Variable	Solution	Units
Beam Quality	2	-
Aperture Size	70	cm (diameter)
Wavelength	1.03	μm
Slant Range	11	Km
HEL Power	400	kW

When in a vacuum, beam quality is best at 1, however it appears when in the company of other parameters and atmospheric variations, that value is not ideal. A larger aperture size will typically yield a tighter, smaller, more focused beam on target. We identified a possible relationship between aperture and beam quality; it may be these parameters in combination make PIB best achievable when beam quality is 1 and aperture size is at its largest. Smaller wavelengths are known to be less effected by absorption and scattering, due to their faster travel time through the atmosphere, and lower index of refraction. Lower wavelengths can be chosen to reduce absorption and scattering effects, allowing other parameters that do cause absorption and scattering, like power, to be set higher. Higher powers are always more affected by absorption, scattering, and turbulence effects, however it is typically worth the price. A laser beam may spread, bend, get absorbed by the atmosphere, etc., but if enough of the intensity survives despite losses along the way, it could still cause severe damage to a target with what remains. This appears to be the case for the solution found. A slant range of 11 km is not surprising, given the shorter distance a beam has to propagate, the less atmospheric effects encountered along the way.

4.4 Summary

Even without satisfying normality of residuals and constant variance of the full empirical model of the Air-to-Ground engagement, in a practical sense, inferences can be made regarding parameters significant in explaining variations to PIB. After

removing select influential points associated with extreme atmospheric visibility conditions, normality of residuals and constant variance was achieved. In a practical sense, HEL test would not be conducted on days with poor visibility, however, capturing poor weather days to modeling can provide valuable insights to system limitations.

V. Conclusions and Recommendations

5.1 Summary of Key Contributions

Two key contributions were made by this research: applying DOE and RSM to modeling an HEL weapon system engagement, and incorporating atmospheric variation into performance modeling, enabling objective inferences of significant effects to be made.

The application of DOE is prevalent in live testing, however this research shows it can effectively and efficiently be applied to modeling and simulation of conceptual or existing systems. Modeling and simulation provides a cost effective and resource efficient alternative to live testing, allowing system parameter relationships and key drivers of system performance to be assessed with high confidence, without ever conducting a live test. The experimental factorial test design used in this thesis took five factors and varied them at different levels simultaneously, allowing not only main effects to be analyzed, but also interactions and nonlinear effects. Results found that many interactions and nonlinear effects had both practical and statistical significance, which suggest evidence that these relationships drive performance, and it is important they be modeled.

Nuisance factors are modeled stochastically in this research, which enables residual analysis to be conducted. This is done by incorporating actual weather observations from meteorological reports, varied turbulence, and varied jitter into the HEL propagation model. Each factorial design point is ran three times (replicated), with these effects being varied for each run. There are two advantages to modeling a stochastic nuisance factors: first, it captures variations in system performance as a function of atmospheric conditions and platform jitter, and second, enables us trace units variation of the response back to design factors of interest.

5.2 Key Findings

Residuals from the full empirical model (which is composed of main, interaction, and non-linear effects), were analyzed and failed to be normally

distributed with constant variance. Statistical inferences could not be made from this model. However, given a factor explained three times the magnitude of variation to the response as error, the factor has practical significance, as it's highly unlikely units of variation that large are caused by error.

The source of influential points were assessed and traced back to METAR observations which included very poor atmospheric visibility observations. Observations with visibility less than 16 statute miles had a severe effect on HEL beam propagation. These influential points were removed from the model, and a new empirical model was assessed. Residuals were normally distributed with constant variance. Since model adequacy was achieved, statistical inferences could be drawn.

Table 11 compares the two empirical models examined; one with poor atmospheric visibility cases included, and the other with them removed. From both models, the most significant contributors are slant range, HEL power, and aperture size, the interaction of slant range and power, and the nonlinear term of power squared. These three parameters explain a large portion of the variation caused to power in bucket. The actual experimental design with associated power in bucket values are listed in appendix D.

Table 11: Model Comparisons - With and Without Poor Visibility Conditions

	Full Model		Full Model w/Points Removed		
Source	Sum of Squares	F Ratio	Sum of Squares	F Ratio	Value
Slant Range	4.19E+11	1267.423	1317971.8	3642.304	<.0001*
Power	1.03E+11	311.6151	282437.6	780.5353	<.0001*
Aperture	6.57E+10	198.8881	224666.1	620.8799	<.0001*
Slant Range*Power	5.95E+10	180.1317	81830.6	226.1444	<.0001*
Slant Range*Slant Range	2.05E+10	62.0959	25217.5	69.6901	<.0001*
Aperture*Power	1.15E+10	34.7226	13719.8	37.9156	<.0001*
Power*Power	6.453E+09	19.535	17920.8	49.5253	<.0001*
Wavelength*Wavelength	6.445E+09	19.5106	14307.3	39.5393	<.0001*
Wavelength	5.514E+09	16.6935	24561.1	67.8761	<.0001*
Beam Quality	5.003E+09	15.1445	16995.4	46.968	<.0001*
Wavelength*Power	2.969E+09	8.9893	5510.7	15.2292	0.0001*
Beam Quality*Slant Range	2.474E+09	7.4905	2658.5	7.3468	0.0072*
Beam Quality*Aperture	2.184E+09	6.6121	6361.8	17.5813	<.0001*
Aperture*Slant Range	890092915	2.6946	3528.3	9.7506	0.0020*
Beam Quality*Power	725628346	2.1967	3288.4	9.0876	0.0028*
Beam Quality*Wavelength	178779336	0.5412	240.9	0.6657	0.4153
Aperture*Wavelength	120594590	0.3651	318.6	0.8805	0.3489
Wavelength*Slant Range	104485318	0.3163	1349.1	3.7283	0.0546
Beam Quality*Beam Quality	58002324	0.1756	352.2	0.9735	0.3247
Aperture*Aperture	23437258	0.071	6236.1	17.234	<.0001*

The factors are ordered by the size of associated F-ratios. The two models order the factors of significance in the same order, up until to the 13th effects, Aperture*Slant Range. Main, interaction, and nonlinear effects depict significance, thus RSM is used to analyze the response surface. Nonlinear and interaction effects of significance listed in Table 11 were examined. Justifications for these nonlinear relationships are likely due to thermal blooming effects. The full empirical model was assessed using thermal blooming as a response, and the three largest contributors to variation in thermal blooming were power, aperture size, and slant

range. These three factors had the most non-linear and interactions significance as seen in the full model, when using PIB as response.

Response surface analysis was used for this research and unveiled many interactions and non-linear effects that exist among the design factors selected. Capturing these effects within an empirical model allows us to better estimate and predict HEL performance.

5.3 Caveats on Research

HEELEOS has not formally been verified, validated, and accredited, however it is an HEL propagation model widely accepted and used across DoD Joint Services (Army, Navy, and Air Force) for Directed Energy Modeling and Simulation. It is often used in conjunction with the wave optics code, WaveTrain, to which it is anchored. In regards to the accuracy of METAR data, reports were collected from two sources and compared. Both sources captured identical observations for Dayton, OH, the geographic location selected for this research.

5.4 Recommendations for Future Work

DOE is not just a methodology used for system level modeling. HEL systems are highly complex, and DOE applications at the sub-system level could provide valuable insights about cost-benefit relationships in the form of weight and volume versus performance gain. These relationships were never examined in this thesis, but would play a very important role in the function and design of any laser weapon system.

A follow on to this research could examine the empirical model based on actual HEL tests. Conclusions based on RSM could be compared to model and simulation results. This iterative process could help improve the predictive capability of current HEL models.

5.5 Implications for Directed Energy Testing

HEELEOS is an accepted credible model. We found strong nonlinear effects between the factors controlled and the response of interest. A one-factor-at-a-time

(OFAT) test would not have been able to estimate the nonlinear model. Those nonlinear effects would have been left in error, thus overstating error, and obscuring the results. Live testing in the DE domain should consider moving away from OFAT and adapt DOE as a methodology for achieving greater efficiency and effectiveness in test by actually modeling the nonlinear response function.

Appendix A. $3^{4-1}4^1$ Fractional Experimental Design

Below is the $3^{4-1}4^1$ Fractional Experimental Design. This design is replicated 3 times with each model.

$3^{4-1}4^1$ Experimental Design with 108 Design Points					
Order	Beam Quality	Aperture (cm)	Wavelength (μm)	Slant Range (km)	Power (kW)
1	1	70	1.045	11	250
2	2	30	1.064	17	400
3	1	70	1.064	25	150
4	1	30	1.064	17	250
5	2	30	1.045	11	250
6	1.5	50	1.030	17	250
7	1	30	1.030	25	100
8	2	70	1.030	11	400
9	2	30	1.064	17	150
10	1	30	1.030	11	250
11	1	30	1.045	25	100
12	1.5	30	1.064	25	100
13	1.5	50	1.045	17	150
14	1	30	1.064	17	150
15	1	50	1.045	11	250
16	1.5	30	1.030	11	400
17	1.5	70	1.045	25	150
18	2	70	1.064	25	400
19	1.5	50	1.045	17	150
20	1.5	70	1.045	17	250
21	1	70	1.030	17	250
22	1	50	1.030	11	400
23	1.5	30	1.045	25	150
24	1.5	30	1.045	25	250
25	1.5	50	1.064	11	250
26	2	50	1.045	25	250
27	1	50	1.045	11	400
28	2	50	1.030	25	400
29	1	30	1.064	17	100
30	1.5	50	1.030	11	100
31	1	30	1.045	11	400
32	1	30	1.064	25	250
33	1.5	50	1.064	11	150
34	2	70	1.030	17	100
35	1	70	1.030	11	100
36	1	30	1.045	11	150
37	2	30	1.045	17	250
38	2	50	1.045	25	250
39	1.5	50	1.064	25	250

Order	Beam Quality	Aperture (cm)	Wavelength (μm)	Slant Range (km)	Power (kW)
40	1.5	30	1.064	25	100
41	1.5	70	1.045	25	400
42	1	50	1.045	25	100
43	2	30	1.045	17	150
44	2	70	1.064	11	100
45	1.5	70	1.045	11	100
46	2	50	1.030	17	150
47	2	50	1.045	11	150
48	1	70	1.045	17	100
49	2	70	1.064	25	100
50	1	70	1.045	17	400
51	1.5	50	1.030	25	150
52	2	70	1.064	25	150
53	1.5	30	1.064	11	400
54	1	70	1.030	11	150
55	2	30	1.045	25	400
56	1	50	1.030	25	100
57	2	70	1.045	11	150
58	1	70	1.064	11	150
59	2	30	1.045	11	100
60	2	30	1.045	25	400
61	1	50	1.045	17	100
62	2	50	1.064	25	100
63	1	30	1.030	25	250
64	2	70	1.030	11	250
65	2	30	1.030	11	150
66	1.5	30	1.045	17	100
67	2	70	1.030	25	150
68	2	70	1.030	11	250
69	1	70	1.045	25	150
70	1.5	30	1.030	11	150
71	2	50	1.064	17	150
72	2	30	1.064	11	100
73	1	30	1.030	17	400
74	1	50	1.064	17	400
75	1	50	1.064	17	150
76	2	70	1.064	11	400
77	1.5	30	1.064	11	150
78	1.5	30	1.030	25	150
79	1.5	50	1.045	11	100
80	2	50	1.064	17	400
81	1	30	1.064	25	250
82	1.5	70	1.064	11	250
83	1.5	50	1.064	11	250
84	2	70	1.030	25	250
85	2	30	1.030	17	250
86	1.5	30	1.030	17	400
87	1	70	1.030	25	100

Order	Beam Quality	Aperture (cm)	Wavelength(μm)	Slant Range (km)	Power (kW)
88	1.5	70	1.064	25	400
89	1.5	50	1.030	17	250
90	2	50	1.030	17	100
91	1.5	70	1.045	25	400
92	1.5	70	1.045	17	400
93	2	50	1.064	17	100
94	2	70	1.045	17	250
95	1.5	70	1.064	17	250
96	1	50	1.045	11	400
97	1.5	30	1.030	17	400
98	1	50	1.030	25	150
99	1.5	70	1.030	17	100
100	1.5	50	1.030	25	400
101	1	50	1.064	25	250
102	2	50	1.030	25	400
103	1	70	1.064	17	400
104	1	50	1.064	11	400
105	1	70	1.030	17	150
106	1.5	30	1.030	11	100
107	2	50	1.045	11	100
108	1.5	70	1.064	17	100

Appendix B. LEEDR Varied Inputs (Experimental Design & Nuisance Factors)

Below is the table of data used to enter variations in design points and nuisance factors into LEEDR. There were 108 design points, replicated 3 times. Each replication called for a unique atmospheric profile.

Design Point Column Headings:

BQ = Beam Quality

AP = Aperture Diameter (cm)

WL = Wavelength (μm)

SR = Slant Range (km)

PW = HEL Output Power (kW)

Replication Column Headings:

A = Earth Surface Visibility (km)

B = Wind at Earth Surface (m/s)

C = Wind Direction (0 = North)

D = Temp @ Earth's Surface (F)

E = Dew Point @ Earth's Surface (F)

	Design Points					Replication I					Replication II					Replication III				
	BQ	AP	WL	SR	PW	A	B	C	D	E	A	B	C	D	E	A	B	C	D	E
1	1	70	1.045	11	250	16.1	4.6	100	71.6	46.4	16.1	5.1	240	89.6	69.8	16.1	4.1	260	87.8	77
2	2	30	1.064	17	400	16.1	3.1	230	78.8	60.8	11.3	4.1	120	69.8	64.4	16.1	5.1	350	69.8	53.6
3	1	70	1.064	25	150	16.1	3.1	200	86	71.6	16.1	2.6	10	80.6	60.8	16.1	4.6	250	82.4	69.8
4	1	30	1.064	17	250	16.1	2.6	70	77	60.8	16.1	3.6	110	73.4	69.8	16.1	4.6	20	77	53.6
5	2	30	1.045	11	250	16.1	2.6	40	64.4	60.8	16.1	2.1	310	77	60.8	16.1	2.1	80	68	68
6	1.5	50	1.030	17	250	16.1	3.1	100	78.8	66.2	16.1	3.1	320	75.2	66.2	16.1	3.1	290	77	69.8
7	1	30	1.030	25	100	16.1	4.6	180	71.6	66.2	16.1	0.0	0	78.8	71.6	9.7	3.6	240	73.4	73.4
8	2	70	1.030	11	400	16.1	3.6	240	86	69.8	16.1	3.6	180	82.4	73.4	16.1	2.6	250	80.6	69.8
9	2	30	1.064	17	150	16.1	4.6	220	80.6	68	16.1	3.6	100	80.6	60.8	16.1	0.0	0	78.8	62.6
10	1	30	1.030	11	250	16.1	5.7	320	75.2	62.6	16.1	4.6	40	80.6	60.8	16.1	5.1	210	73.4	69.8
11	1	30	1.045	25	100	16.1	2.6	0	73.4	50	16.1	7.2	260	89.6	75.2	16.1	5.1	360	71.6	51.8
12	1.5	30	1.064	25	100	16.1	2.1	210	82.4	62.6	6.4	3.6	40	66.2	59	16.1	6.2	230	80.6	59
13	1.5	50	1.045	17	150	16.1	7.2	300	80.6	69.8	16.1	5.1	320	68	48.2	16.1	2.1	150	73.4	69.8
14	1	30	1.064	17	150	16.1	3.1	40	73.4	51.8	16.1	4.6	180	80.6	66.2	16.1	5.1	290	78.8	68
15	1	50	1.045	11	250	16.1	7.7	280	77	51.8	16.1	2.6	340	78.8	66.2	16.1	3.1	60	71.6	57.2
16	1.5	30	1.030	11	400	9.7	0.0	0	69.8	66.2	11.3	4.1	310	86	66.2	11.3	5.1	230	64.4	64.4
17	1.5	70	1.045	25	150	6.4	1.5	270	66.2	62.6	16.1	3.6	360	77	66.2	16.1	2.6	110	77	57.2
18	2	70	1.064	25	400	16.1	2.1	30	75.2	50	16.1	4.6	200	91.4	57.2	16.1	3.6	10	80.6	64.4
19	1.5	50	1.045	17	150	16.1	5.1	140	77	55.4	16.1	3.1	80	78.8	64.4	16.1	2.1	90	77	62.6
20	1.5	70	1.045	17	250	16.1	3.1	240	84.2	68	16.1	1.5	130	69.8	57.2	16.1	3.1	300	86	77
	Design Point					Replication I					Replication II					Replication III				

	BQ	AP	WL	SR	PW	A	B	C	D	E	A	B	C	D	E	A	B	C	D	E
21	1	70	1.030	17	250	16.1	3.6	220	75.2	60.8	16.1	4.6	190	84.2	64.4	16.1	3.1	230	82.4	68
22	1	50	1.030	11	400	16.1	10.3	230	77	62.6	16.1	5.7	70	73.4	46.4	16.1	3.1	250	84.2	68
23	1.5	30	1.045	25	150	16.1	6.2	70	77	64.4	16.1	0.0	0	82.4	60.8	16.1	6.2	330	62.6	55.4
24	1.5	30	1.045	25	250	6.4	6.7	10	59	55.4	16.1	2.1	330	71.6	57.2	16.1	4.1	220	84.2	71.6
25	1.5	50	1.064	11	250	16.1	0.0	0	73.4	53.6	16.1	1.0	40	80.6	64.4	16.1	0.0	0	77	51.8
26	2	50	1.045	25	250	16.1	2.1	90	69.8	60.8	16.1	2.1	280	80.6	69.8	16.1	6.7	310	69.8	55.4
27	1	50	1.045	11	400	16.1	4.6	250	75.2	59	16.1	2.1	60	78.8	69.8	16.1	5.1	230	84.2	68
28	2	50	1.030	25	400	16.1	7.2	250	89.6	75.2	16.1	3.6	270	71.6	59	16.1	1.5	350	80.6	62.6
29	1	30	1.064	17	100	16.1	2.6	280	87.8	71.6	16.1	2.1	290	77	68	16.1	4.1	320	71.6	62.6
30	1.5	50	1.030	11	100	16.1	4.1	260	91.4	77	16.1	3.6	250	77	57.2	3.2	7.2	230	68	66.2
31	1	30	1.045	11	400	16.1	3.6	350	77	55.4	16.1	2.1	320	77	66.2	16.1	5.1	210	82.4	68
32	1	30	1.064	25	250	16.1	3.1	270	75.2	69.8	16.1	5.7	50	75.2	60.8	16.1	2.1	340	71.6	60.8
33	1.5	50	1.064	11	150	16.1	4.6	200	91.4	77	16.1	0.0	0	75.2	66.2	16.1	3.6	290	89.6	78.8
34	2	70	1.030	17	100	16.1	3.6	270	86	68	16.1	4.1	290	64.4	55.4	16.1	2.6	200	86	66.2
35	1	70	1.030	11	100	16.1	3.1	200	73.4	68	16.1	6.7	240	82.4	73.4	16.1	3.1	250	78.8	69.8
36	1	30	1.045	11	150	16.1	2.6	340	86	71.6	16.1	2.6	10	78.8	55.4	16.1	3.6	350	82.4	51.8
37	2	30	1.045	17	250	16.1	0.0	0	78.8	68	16.1	2.1	260	73.4	53.6	16.1	4.1	310	78.8	68
38	2	50	1.045	25	250	16.1	4.6	20	78.8	62.6	16.1	0.0	0	73.4	60.8	16.1	3.6	350	77	57.2
39	1.5	50	1.064	25	250	16.1	0.0	0	82.4	66.2	16.1	2.1	190	82.4	66.2	16.1	2.6	40	80.6	64.4
40	1.5	30	1.064	25	100	16.1	2.6	250	86	68	16.1	2.1	290	84.2	64.4	16.1	3.1	340	80.6	68
41	1.5	70	1.045	25	400	16.1	5.1	220	77	62.6	9.7	5.1	240	80.6	69.8	8.0	3.1	110	66.2	64.4
42	1	50	1.045	25	100	16.1	1.5	0	80.6	66.2	16.1	1.5	330	73.4	60.8	16.1	6.2	230	75.2	68
43	2	30	1.045	17	150	16.1	5.7	230	78.8	73.4	16.1	4.6	250	86	71.6	16.1	7.2	230	78.8	57.2
44	2	70	1.064	11	100	16.1	6.7	250	77	62.6	16.1	3.1	20	71.6	64.4	16.1	3.1	240	78.8	59
45	1.5	70	1.045	11	100	16.1	3.1	50	73.4	57.2	16.1	4.1	200	66.2	66.2	16.1	1.5	20	75.2	64.4
46	2	50	1.030	17	150	16.1	5.7	290	82.4	55.4	16.1	6.7	40	64.4	42.8	16.1	0.0	0	77	50
47	2	50	1.045	11	150	16.1	5.7	210	75.2	71.6	16.1	5.1	340	62.6	55.4	12.9	5.1	200	75.2	73.4
48	1	70	1.045	17	100	16.1	5.1	340	69.8	55.4	16.1	3.6	50	68	50	16.1	8.7	230	75.2	62.6
49	2	70	1.064	25	100	16.1	5.7	70	69.8	59	16.1	4.6	250	75.2	69.8	16.1	2.1	290	80.6	59
50	1	70	1.045	17	400	16.1	5.1	250	77	71.6	16.1	2.1	290	82.4	66.2	14.5	1.5	240	80.6	68
51	1.5	50	1.030	25	150	16.1	0.0	0	78.8	60.8	11.3	4.1	120	69.8	64.4	16.1	3.1	20	71.6	51.8
52	2	70	1.064	25	150	16.1	4.1	90	66.2	50	16.1	6.2	270	82.4	68	16.1	4.6	220	84.2	69.8
53	1.5	30	1.064	11	400	16.1	5.1	290	89.6	78.8	16.1	3.6	300	80.6	73.4	16.1	1.5	160	71.6	59
54	1	70	1.030	11	150	16.1	7.2	240	77	60.8	16.1	6.2	310	80.6	66.2	16.1	3.6	50	73.4	48.2
Design Points						Replication I					Replication II					Replication III				

	BQ	AP	WL	SR	PW	A	B	C	D	E	A	B	C	D	E	A	B	C	D	E
55	2	30	1.045	25	400	16.1	2.1	280	80.6	69.8	16.1	5.1	10	73.4	59	16.1	3.6	210	80.6	66.2
56	1	50	1.030	25	100	16.1	3.6	360	78.8	69.8	16.1	4.6	10	77	50	16.1	3.1	230	82.4	73.4
57	2	70	1.045	11	150	16.1	2.1	310	71.6	68	16.1	2.6	270	80.6	64.4	11.3	5.7	220	64.4	64.4
58	1	70	1.064	11	150	16.1	2.6	350	75.2	57.2	16.1	5.1	50	84.2	59	16.1	4.1	280	71.6	60.8
59	2	30	1.045	11	100	16.1	6.7	330	62.6	55.4	16.1	5.1	230	86	68	16.1	2.6	110	68	44.6
60	2	30	1.045	25	400	16.1	4.1	20	77	59	16.1	4.1	60	75.2	48.2	16.1	0.0	0	84.2	75.2
61	1	50	1.045	17	100	16.1	3.6	190	82.4	64.4	9.7	5.1	260	75.2	69.8	16.1	3.1	320	64.4	57.2
62	2	50	1.064	25	100	16.1	4.1	240	84.2	73.4	16.1	5.7	320	80.6	50	16.1	4.6	330	71.6	59
63	1	30	1.030	25	250	11.3	6.2	230	77	64.4	16.1	3.6	150	84.2	68	8.0	0.0	0	69.8	69.8
64	2	70	1.030	11	250	16.1	3.1	220	68	51.8	9.7	2.1	270	77	71.6	16.1	5.7	230	80.6	66.2
65	2	30	1.030	11	150	16.1	2.6	40	75.2	53.6	16.1	3.1	30	80.6	62.6	16.1	4.6	100	69.8	51.8
66	1.5	30	1.045	17	100	16.1	4.1	360	84.2	71.6	16.1	4.1	320	69.8	53.6	16.1	3.1	40	73.4	64.4
67	2	70	1.030	25	150	16.1	3.1	340	80.6	71.6	16.1	3.1	320	77	57.2	16.1	2.1	0	82.4	66.2
68	2	70	1.030	11	250	16.1	5.1	250	78.8	64.4	16.1	1.5	100	68	68	16.1	4.6	140	71.6	68
69	1	70	1.045	25	150	16.1	0.0	0	80.6	64.4	16.1	5.1	330	71.6	59	16.1	5.7	110	69.8	64.4
70	1.5	30	1.030	11	150	16.1	6.2	230	86	69.8	16.1	5.7	280	66.2	50	16.1	4.1	60	71.6	51.8
71	2	50	1.064	17	150	16.1	3.1	250	75.2	66.2	16.1	4.1	230	78.8	71.6	16.1	3.6	240	78.8	66.2
72	2	30	1.064	11	100	16.1	4.1	80	80.6	59	16.1	5.1	270	84.2	73.4	16.1	2.6	230	71.6	59
73	1	30	1.030	17	400	16.1	3.1	260	69.8	55.4	8.0	3.1	330	62.6	59	16.1	3.6	340	69.8	53.6
74	1	50	1.064	17	400	16.1	3.6	300	62.6	51.8	16.1	3.1	320	78.8	62.6	16.1	4.6	20	78.8	62.6
75	1	50	1.064	17	150	16.1	5.1	20	77	64.4	16.1	3.1	320	68	55.4	16.1	2.1	300	68	57.2
76	2	70	1.064	11	400	16.1	2.6	310	73.4	59	16.1	3.1	310	78.8	66.2	16.1	7.7	340	69.8	59
77	1.5	30	1.064	11	150	16.1	3.1	260	78.8	64.4	16.1	2.1	40	77	55.4	6.4	7.2	230	73.4	71.6
78	1.5	30	1.030	25	150	16.1	0.0	0	84.2	75.2	16.1	2.1	100	60.8	55.4	16.1	0.0	0	69.8	68
79	1.5	50	1.045	11	100	16.1	0.0	0	84.2	73.4	16.1	2.6	230	80.6	55.4	16.1	5.7	230	84.2	73.4
80	2	50	1.064	17	400	16.1	4.1	240	82.4	68	4.8	4.1	90	73.4	71.6	9.7	4.6	180	80.6	73.4
81	1	30	1.064	25	250	16.1	0.0	0	75.2	59	16.1	3.6	250	78.8	68	16.1	7.7	230	71.6	68
82	1.5	70	1.064	11	250	16.1	5.1	240	73.4	66.2	16.1	1.5	40	75.2	59	16.1	8.7	240	73.4	68
83	1.5	50	1.064	11	250	16.1	3.1	330	71.6	64.4	8.0	2.6	350	84.2	73.4	16.1	3.1	130	71.6	50
84	2	70	1.030	25	250	16.1	1.5	150	75.2	62.6	16.1	2.6	240	77	59	16.1	3.1	60	77	68
85	2	30	1.030	17	250	16.1	2.6	240	78.8	69.8	16.1	0.0	0	68	62.6	16.1	2.6	20	66.2	51.8
86	1.5	30	1.030	17	400	16.1	0.0	0	75.2	68	16.1	3.6	230	71.6	68	16.1	3.1	210	78.8	71.6
87	1	70	1.030	25	100	16.1	2.6	90	89.6	64.4	16.1	3.6	320	69.8	64.4	16.1	3.1	180	78.8	55.4
88	1.5	70	1.064	25	400	16.1	3.1	70	71.6	57.2	16.1	7.2	270	78.8	57.2	16.1	3.1	290	75.2	59
Design Points						Replication I					Replication II					Replication III				

	BQ	AP	WL	SR	PW	A	B	C	D	E	A	B	C	D	E	A	B	C	D	E
89	1.5	50	1.030	17	250	16.1	4.1	200	80.6	60.8	16.1	0.0	0	73.4	66.2	11.3	0.0	0	75.2	60.8
90	2	50	1.030	17	100	9.7	0.0	0	77	71.6	16.1	1.5	360	78.8	66.2	16.1	4.1	240	89.6	71.6
91	1.5	70	1.045	25	400	16.1	2.6	270	84.2	62.6	16.1	4.6	180	73.4	60.8	16.1	5.1	330	75.2	48.2
92	1.5	70	1.045	17	400	16.1	4.1	350	69.8	55.4	16.1	5.1	130	66.2	59	16.1	3.1	270	80.6	71.6
93	2	50	1.064	17	100	16.1	5.1	270	87.8	64.4	16.1	1.5	340	77	64.4	9.7	4.1	270	78.8	73.4
94	2	70	1.045	17	250	16.1	4.1	220	75.2	68	16.1	3.6	220	78.8	68	16.1	5.1	20	78.8	51.8
95	1.5	70	1.064	17	250	16.1	7.2	200	86	69.8	6.4	1.5	290	69.8	66.2	16.1	4.1	250	80.6	64.4
96	1	50	1.045	11	400	0.8	3.6	90	71.6	71.6	16.1	2.1	110	84.2	64.4	16.1	4.6	220	77	62.6
97	1.5	30	1.030	17	400	16.1	7.2	270	86	73.4	16.1	5.7	260	86	77	16.1	3.1	160	84.2	66.2
98	1	50	1.030	25	150	16.1	4.1	250	77	60.8	16.1	3.6	300	75.2	55.4	16.1	4.1	250	80.6	64.4
99	1.5	70	1.030	17	100	16.1	3.6	300	86	62.6	16.1	6.2	240	86	73.4	16.1	4.1	290	78.8	66.2
100	1.5	50	1.030	25	400	16.1	6.7	20	80.6	62.6	16.1	4.6	250	78.8	71.6	16.1	3.6	260	84.2	60.8
101	1	50	1.064	25	250	16.1	4.1	60	71.6	64.4	16.1	3.1	20	73.4	50	16.1	1.5	200	77	66.2
102	2	50	1.030	25	400	16.1	3.6	290	78.8	66.2	16.1	4.6	20	75.2	68	4.8	3.1	270	77	73.4
103	1	70	1.064	17	400	16.1	3.6	100	77	53.6	16.1	4.1	100	69.8	60.8	16.1	2.1	150	77	53.6
104	1	50	1.064	11	400	16.1	6.2	310	77	60.8	16.1	3.1	200	80.6	75.2	16.1	4.1	330	80.6	69.8
105	1	70	1.030	17	150	16.1	3.6	80	77	57.2	16.1	2.6	260	77	62.6	16.1	6.7	240	73.4	68
106	1.5	30	1.030	11	100	16.1	5.1	250	86	64.4	6.4	0.0	0	69.8	69.8	16.1	2.1	170	84.2	73.4
107	2	50	1.045	11	100	11.3	0.0	0	87.8	73.4	16.1	2.1	240	84.2	66.2	16.1	4.1	280	75.2	64.4
108	1.5	70	1.064	17	100	16.1	5.1	30	62.6	60.8	16.1	1.5	100	77	64.4	11.3	0.0	0	77	68

Appendix C. Turbulence and Jitter Variable Inputs into HELEEOS

Below all 108 design points are listed with their corresponding turbulence multiplier and platform jitter inputs.

Design Point Column Headings:

BQ = Beam Quality

AP = Aperture Diameter (cm)

WL = Wavelength (μm)

SR = Slant Range (km)

PW = HEL Output Power (kW)

Replication Column Headings:

TB = Turbulence Multiplier

JR = Platform Jitter Input (μrad)

Experimental Design						Rep I		Rep II		Rep III	
	BQ	AP	WL	SR	PW	TB	JR	TB	JT	TB	JT
1	1	70	1.045	11	250	1.0	1.2	1.7	0.9	0.9	1.3
2	2	30	1.064	17	400	2.2	0.9	2.3	0.7	0.7	1.0
3	1	70	1.064	25	150	2.6	1.0	1.6	1.1	0.8	1.0
4	1	30	1.064	17	250	1.1	1.1	1.0	0.9	0.8	0.7
5	2	30	1.045	11	250	1.7	1.1	1.0	0.7	0.8	0.8
6	1.5	50	1.030	17	250	1.2	1.2	0.7	1.2	0.8	1.0
7	1	30	1.030	25	100	3.5	1.0	1.0	1.1	1.0	1.0
8	2	70	1.030	11	400	1.5	0.9	1.1	0.9	0.7	1.2
9	2	30	1.064	17	150	1.0	0.7	1.4	1.0	1.0	0.9
10	1	30	1.030	11	250	0.6	1.1	0.4	1.1	1.6	0.9
11	1	30	1.045	25	100	1.5	0.8	2.1	0.9	0.2	1.2
12	1.5	30	1.064	25	100	1.8	1.2	0.3	1.1	0.8	0.9
13	1.5	50	1.045	17	150	0.5	0.9	1.0	1.2	1.0	1.1
14	1	30	1.064	17	150	2.3	1.1	2.7	1.0	0.6	0.9
15	1	50	1.045	11	250	3.8	0.9	1.0	1.0	1.4	1.2
16	1.5	30	1.030	11	400	0.3	1.0	0.2	1.0	2.2	0.9
17	1.5	70	1.045	25	150	1.9	1.3	1.1	0.9	1.4	0.9
Experimental Design						Rep I		Rep II		Rep III	

	BQ	AP	WL	SR	PW	TB	JR	TB	JT	TB	JT
18	2	70	1.064	25	400	0.6	1.3	1.7	1.3	1.1	1.1
19	1.5	50	1.045	17	150	0.6	1.0	0.8	1.1	4.2	0.9
20	1.5	70	1.045	17	250	2.4	1.1	1.5	1.2	0.8	0.8
21	1	70	1.030	17	250	1.2	1.0	0.7	1.1	1.0	1.1
22	1	50	1.030	11	400	3.5	1.1	1.8	0.8	1.0	1.0
23	1.5	30	1.045	25	150	2.7	0.9	0.3	1.0	1.3	0.9
24	1.5	30	1.045	25	250	0.8	1.3	1.3	1.3	3.2	0.9
25	1.5	50	1.064	11	250	1.6	0.9	1.4	1.2	0.4	0.8
26	2	50	1.045	25	250	3.2	1.0	0.3	1.1	2.3	1.1
27	1	50	1.045	11	400	1.5	0.6	1.3	1.1	1.5	0.8
28	2	50	1.030	25	400	0.5	1.3	1.7	0.9	0.7	1.2
29	1	30	1.064	17	100	1.9	1.1	3.9	1.4	1.4	1.2
30	1.5	50	1.030	11	100	2.4	1.0	1.5	0.9	4.6	1.0
31	1	30	1.045	11	400	1.9	0.9	1.2	0.9	4.8	0.6
32	1	30	1.064	25	250	6.2	0.4	1.5	0.7	0.5	1.1
33	1.5	50	1.064	11	150	2.6	1.3	0.6	0.8	0.4	1.1
34	2	70	1.030	17	100	0.7	0.9	0.5	1.3	8.8	1.3
35	1	70	1.030	11	100	1.2	0.8	0.8	0.7	1.3	1.2
36	1	30	1.045	11	150	0.7	1.0	1.1	0.8	1.2	1.2
37	2	30	1.045	17	250	3.3	0.9	2.2	1.3	1.6	1.1
38	2	50	1.045	25	250	1.2	0.8	1.2	1.2	1.9	0.9
39	1.5	50	1.064	25	250	3.9	0.5	2.1	0.8	0.3	0.4
40	1.5	30	1.064	25	100	0.8	0.7	0.5	1.1	0.8	1.1
41	1.5	70	1.045	25	400	5.4	0.8	2.2	1.0	1.7	1.1
42	1	50	1.045	25	100	0.3	0.8	5.7	1.2	2.0	0.9
43	2	30	1.045	17	150	1.6	1.4	0.2	0.9	1.6	0.9
44	2	70	1.064	11	100	2.3	0.9	3.4	1.0	1.5	1.3
45	1.5	70	1.045	11	100	2.2	0.9	5.3	0.9	1.4	1.1
46	2	50	1.030	17	150	1.0	1.0	0.6	1.2	1.5	1.2
47	2	50	1.045	11	150	1.2	1.2	3.2	1.1	1.1	0.6
48	1	70	1.045	17	100	1.2	1.3	1.2	1.3	0.4	0.7
Experimental Design						Rep I		Rep II		Rep III	

	BQ	AP	WL	SR	PW	TB	JR	TB	JT	TB	JT
49	2	70	1.064	25	100	0.4	0.9	0.6	11	1.0	1.3
50	1	70	1.045	17	400	2.0	1.1	1.6	0.9	0.9	1.1
51	1.5	50	1.030	25	150	0.5	0.9	1.0	1.1	0.6	1.2
52	2	70	1.064	25	150	1.5	1.0	0.2	1.1	1.7	0.8
53	1.5	30	1.064	11	400	1.2	1.0	0.7	0.7	0.4	0.9
54	1	70	1.030	11	150	2.8	0.8	1.5	1.0	1.0	1.1
55	2	30	1.045	25	400	3.0	1.2	1.5	0.6	1.4	1.0
56	1	50	1.030	25	100	1.3	1.3	1.2	0.8	1.0	0.8
57	2	70	1.045	11	150	3.1	1.1	1.0	1.0	0.5	1.1
58	1	70	1.064	11	150	2.0	1.0	1.3	1.3	2.7	1.2
59	2	30	1.045	11	100	4.5	0.8	2.5	1.0	1.1	0.5
60	2	30	1.045	25	400	1.7	1.3	0.4	1.0	1.5	1.0
61	1	50	1.045	17	100	0.7	1.1	1.2	0.9	0.9	0.8
62	2	50	1.064	25	100	4.1	1.0	2.2	1.1	1.6	0.8
63	1	30	1.030	25	250	1.1	0.7	1.0	1.0	5.2	1.0
64	2	70	1.030	11	250	0.4	1.1	2.0	1.5	0.7	1.1
65	2	30	1.030	11	150	1.4	1.0	1.2	1.2	2.7	1.0
66	1.5	30	1.045	17	100	1.1	1.1	0.8	1.0	0.6	1.1
67	2	70	1.030	25	150	0.9	0.8	0.7	1.1	1.1	0.7
68	2	70	1.030	11	250	1.1	0.8	0.6	1.0	1.8	1.0
69	1	70	1.045	25	150	2.4	1.0	0.8	1.0	0.9	0.8
70	1.5	30	1.030	11	150	2.9	1.5	0.9	1.0	0.7	1.4
71	2	50	1.064	17	150	1.0	1.1	0.3	0.7	0.7	1.0
72	2	30	1.064	11	100	1.0	1.3	2.2	0.7	1.8	0.8
73	1	30	1.030	17	400	1.3	1.3	0.9	1.0	1.0	0.6
74	1	50	1.064	17	400	1.7	0.8	1.0	1.0	0.7	1.2
75	1	50	1.064	17	150	0.8	1.0	1.4	0.9	0.3	1.2
76	2	70	1.064	11	400	2.2	1.1	0.6	0.8	1.9	0.9
77	1.5	30	1.064	11	150	1.7	1.0	1.5	1.0	1.1	1.5
78	1.5	30	1.030	25	150	0.8	1.4	0.8	0.7	0.8	1.2
79	1.5	50	1.045	11	100	2.6	0.9	2.5	1.0	0.4	1.0
Experimental Design						Rep I		Rep II		Rep III	

	BQ	AP	WL	SR	PW	TB	JR	TB	JT	TB	JT
80	2	50	1.064	17	400	2.1	1.2	0.6	1.0	3.0	1.0
81	1	30	1.064	25	250	2.2	1.0	0.5	1.3	1.2	0.9
82	1.5	70	1.064	11	250	0.4	1.0	0.4	0.8	2.5	0.9
83	1.5	50	1.064	11	250	1.9	0.9	1.5	0.8	0.8	1.0
84	2	70	1.030	25	250	2.8	1.2	2.0	1.0	1.0	1.1
85	2	30	1.030	17	250	0.7	1.1	2.9	0.9	1.8	0.8
86	1.5	30	1.030	17	400	1.1	0.8	1.1	1.2	2.6	1.0
87	1	70	1.030	25	100	1.5	1.1	0.4	0.9	1.4	1.2
88	1.5	70	1.064	25	400	1.6	0.8	1.3	1.5	1.4	1.0
89	1.5	50	1.030	17	250	2.0	1.0	4.5	0.9	0.5	0.8
90	2	50	1.030	17	100	1.8	1.0	1.4	1.1	2.2	0.8
91	1.5	70	1.045	25	400	1.1	1.1	2.6	1.2	0.4	0.8
92	1.5	70	1.045	17	400	0.7	1.0	1.2	1.0	3.4	1.0
93	2	50	1.064	17	100	1.8	1.3	7.1	0.8	0.7	1.3
94	2	70	1.045	17	250	1.8	1.2	0.8	1.3	0.9	0.5
95	1.5	70	1.064	17	250	0.8	0.8	1.3	1.0	3.4	1.1
96	1	50	1.045	11	400	1.1	0.9	0.6	0.8	0.4	0.6
97	1.5	30	1.030	17	400	0.7	1.1	0.8	0.8	0.7	1.2
98	1	50	1.030	25	150	3.7	1.4	1.2	0.7	1.9	1.3
99	1.5	70	1.030	17	100	4.1	1.0	0.9	1.1	4.6	1.0
100	1.5	50	1.030	25	400	2.2	1.1	0.5	1.0	0.8	1.0
101	1	50	1.064	25	250	1.5	1.0	2.6	0.9	3.1	0.8
102	2	50	1.030	25	400	2	1.2	0.8	1.3	0.5	1.0
103	1	70	1.064	17	400	1.3	0.8	3.6	0.9	2.6	0.7
104	1	50	1.064	11	400	1.2	0.9	1.8	1.0	1.5	0.6
105	1	70	1.030	17	150	0.8	0.8	0.9	1.0	1.1	0.9
106	1.5	30	1.030	11	100	1.4	1.0	1.0	1.1	2.2	1.0
107	2	50	1.045	11	100	1.1	1.3	1.4	0.8	4.2	0.9
108	1.5	70	1.064	17	100	0.6	1.1	2.8	1.0	1.9	1.2

Appendix D. Design Points with Associated Response Variables

Below is the table of data with 108 design points, replicated 3 times, and the response variables collected from HELEEOS. Responses include HEL path transmittance, thermal blooming effect, average irradiance, and power in bucket.

Design Point Column Headings:

Replication Column Headings:

BQ = Beam Quality

A = Thermal Blooming (km)

AP = Aperture Diameter (cm)

B = Atmospheric Transmittance (km⁻¹)

W = Wavelength (μm)

C = Power in Bucket (Watts)

S = Slant Range (km)

D = Average Irradiance (Watts/cm²)

P = HEL Output Power (kW)

DESIGN POINTS						Rep I				Rep II				Rep III			
	W	S	BQ	AP	P	A	B	C	D	A	B	C	D	A	B	C	D
1	1.045	11	1	70	250	155.8	0.89	175336.94	2233.59	158.3	0.83	172288.69	2194.76	132.2	0.71	167699.49	2136.30
2	1.0642	17	2	30	400	398.2	0.71	40151.16	511.48	295.0	0.51	30637.29	390.28	257.4	0.67	44391.65	565.50
3	1.0642	25	1	70	150	368.6	0.52	27043.85	344.51	284.3	0.65	33405.71	425.55	172.3	0.48	30281.66	385.75
4	1.0642	17	1	30	250	195.9	0.67	45160.36	575.29	176.6	0.48	32403.13	412.78	186.2	0.81	55377.54	705.45
5	1.045	11	2	30	250	87.8	0.62	85396.81	1087.86	103.8	0.78	106901.02	1361.80	102.2	0.60	82221.58	1047.41
6	1.03	17	1.5	50	250	211.2	0.61	77672.32	989.46	179.4	0.54	75395.32	960.45	181.2	0.52	72491.90	923.46
7	1.03	25	1	30	100	167.8	0.36	10339.92	131.72	64.0	0.38	12736.15	162.24	55.4	0.56	19612.89	249.85
8	1.03	11	2	70	400	348.5	0.77	221852.70	2826.15	1047.2	0.67	163441.51	2082.06	341.2	0.70	225481.41	2872.37
9	1.0642	17	2	30	150	133.3	0.61	21914.40	279.16	123.3	0.75	26539.50	338.08	123.5	0.67	25343.18	322.84
10	1.03	11	1	30	250	82.0	0.72	138173.61	1760.17	95.9	0.83	150956.86	1923.02	163.6	0.61	103960.90	1324.34
11	1.045	25	1	30	100	91.3	0.76	22600.08	287.90	45.9	0.52	17149.26	218.46	66.9	0.66	20728.80	264.06
12	1.0642	25	1.5	30	100	162.7	0.65	9722.17	123.85	78.1	0.04	718.17	9.15	104.3	0.69	11022.79	140.42
13	1.045	17	1.5	50	150	66.0	0.59	61684.63	785.79	93.8	0.76	70478.88	897.82	156.6	0.48	45938.19	585.20
14	1.0642	17	1	30	150	123.0	0.78	42828.23	545.58	329.3	0.64	30635.86	390.27	87.3	0.58	34858.77	444.06
15	1.045	11	1	50	250	100.4	0.89	174885.51	2227.84	116.6	0.73	164094.71	2090.38	121.5	0.75	164188.22	2091.57
16	1.03	11	1.5	30	400	195.6	0.46	96447.98	1228.64	313.0	0.62	107668.94	1371.58	126.3	0.80	201356.57	2565.05

DEISGN POINTS						Rep I				Rep II				Rep III			
	W	S	BQ	AP	P	A	B	C	D	A	B	C	D	A	B	C	D
17	1.045	17	1.5	70	150	135.9	0.07	5792.99	73.80	140.3	0.46	40478.18	515.65	199.4	0.66	45241.35	576.32
18	1.0642	25	2	70	400	889.4	0.75	34516.78	439.70	1201.0	0.77	25526.21	325.17	595.4	0.56	42659.79	543.44
19	1.045	17	1.5	50	150	148.8	0.79	63574.04	809.86	102.8	0.65	62893.32	801.19	121.4	0.65	62339.14	794.13
20	1.045	17	1.5	70	250	240.5	0.68	107656.60	1371.42	317.9	0.62	102216.73	1302.12	165.9	0.55	110412.47	1406.53
21	1.03	17	1	70	250	312.5	0.64	99482.35	1267.29	629.0	0.75	68505.57	872.68	305.7	0.64	102153.19	1301.31
22	1.03	11	1	50	400	208.5	0.75	182523.13	2325.14	196.0	0.89	207736.81	2646.33	301.7	0.77	193529.00	2465.34
23	1.045	25	1.5	30	150	68.2	0.49	15056.97	191.81	97.0	0.71	20868.10	265.84	68.9	0.39	12458.02	158.70
24	1.045	25	1.5	30	250	144.0	0.07	2262.67	28.82	177.4	0.53	21012.58	267.68	180.8	0.49	18566.61	236.52
25	1.0642	11	1.5	50	250	145.5	0.83	150240.61	1913.89	236.0	0.77	136074.20	1733.43	145.4	0.88	153254.20	1952.28
26	1.045	25	2	50	250	217.4	0.42	24935.81	317.65	218.4	0.46	27657.66	352.33	154.0	0.53	32934.72	419.55
27	1.045	11	1	50	400	217.5	0.78	207065.56	2637.78	206.0	0.68	207469.45	2642.92	245.9	0.78	194055.66	2472.05
28	1.03	25	2	50	400	309.5	0.51	37115.06	472.80	350.4	0.48	36311.83	462.57	598.1	0.61	41763.29	532.02
29	1.0642	17	1	30	100	77.7	0.67	31108.46	396.29	74.3	0.55	24838.30	316.41	61.1	0.55	26574.92	338.53
30	1.03	11	1.5	50	100	65.7	0.74	70807.18	902.00	72.0	0.83	77644.05	989.10	76.7	0.17	16185.03	206.18
31	1.045	11	1	30	400	143.9	0.86	205737.87	2620.86	153.4	0.71	178137.59	2269.27	232.4	0.75	162686.21	2072.44
32	1.0642	25	1	30	250	201.0	0.37	11124.29	141.71	182.4	0.52	16919.43	215.53	244.7	0.45	13760.49	175.29
33	1.0642	11	1.5	50	150	191.5	0.75	85024.61	1083.12	83.0	0.68	92013.31	1172.14	91.1	0.70	92646.16	1180.21
34	1.03	17	2	70	100	96.5	0.71	55786.39	710.65	68.5	0.55	42085.80	536.12	226.5	0.75	48655.40	619.81
35	1.03	11	1	70	100	134.9	0.63	63156.92	804.55	60.4	0.67	67350.80	857.97	77.6	0.67	67188.28	855.90
36	1.045	11	1	30	150	54.0	0.75	97444.66	1241.33	61.3	0.88	111217.77	1416.79	58.1	0.90	110810.01	1411.59
37	1.045	17	2	30	250	108.9	0.59	39778.39	506.73	172.1	0.76	46116.95	587.48	106.9	0.59	39487.83	503.03
38	1.045	25	2	50	250	205.7	0.57	35968.19	458.19	237.2	0.49	29522.16	376.08	260.9	0.66	32377.21	412.45
39	1.0642	25	1.5	50	250	361.0	0.56	26869.01	342.28	754.5	0.56	22216.75	283.02	333.1	0.56	27299.16	347.76
40	1.0642	25	1.5	30	100	109.3	0.60	10217.36	130.16	111.5	0.65	10793.13	137.49	89.8	0.48	8601.54	109.57
41	1.045	25	1.5	70	400	434.2	0.52	62814.84	800.19	322.3	0.46	60628.45	772.34	341.0	0.32	42562.68	542.20
42	1.045	25	1	50	100	114.4	0.52	28440.89	362.30	105.1	0.49	23091.82	294.16	71.6	0.39	20139.61	256.56
43	1.045	17	2	30	150	74.7	0.51	21564.76	274.71	75.2	0.64	28458.11	362.52	87.0	0.79	33263.31	423.74
44	1.0642	11	2	70	100	66.6	0.75	71706.49	913.46	64.2	0.66	64071.96	816.20	111.9	0.83	74572.22	949.96
45	1.045	11	1.5	70	100	53.6	0.78	77368.39	985.58	101.8	0.60	59043.57	752.15	63.0	0.71	70275.38	895.23
46	1.03	17	2	50	150	107.9	0.84	62324.67	793.94	93.4	0.79	61824.97	787.58	151.4	0.84	60211.47	767.03

DEISGN POI						Rep I			Rep II					Rep III			
	W	S	BQ	AP	P	A	B	C	D	A	B	C	D	A	B	C	D
47	1.045	11	2	50	150	102.80	0.62	77670.89	989.44	52.2	0.66	87279.59	1111.84	113.3	0.66	84576.40	1077.41
48	1.045	17	1	70	100	62.6	0.65	58566.46	746.07	77.3	0.72	63057.66	803.28	61.3	0.62	58190.08	741.27
49	1.0642	25	2	70	100	122.10	0.45	20215.69	257.52	103.3	0.37	15543.46	198.01	190.9	0.69	23586.07	300.46
50	1.045	17	1	70	400	243.50	0.51	125092.65	1593.54	364.4	0.68	141348.01	1800.61	576.2	0.43	111652.77	1422.3
51	1.03	25	1.5	50	150	191.20	0.61	33449.65	426.11	138.1	0.18	9430.22	120.13	179.2	0.65	33246.11	423.52
52	1.0642	25	2	70	150	192.00	0.56	29238.50	372.46	142.3	0.52	29314.75	373.44	233.4	0.52	26411.16	336.45
53	1.0642	11	1.5	30	400	171.40	0.70	124085.19	1580.70	184.7	0.66	117035.65	1490.90	467.7	0.73	113353.42	1443.99
54	1.03	11	1	70	150	89.2	0.77	112669.87	1435.29	89.2	0.77	112389.39	1431.71	93.2	0.89	126839.56	1615.79
55	1.045	25	2	30	400	254.00	0.46	18130.09	230.96	228.1	0.52	22531.84	287.03	348.5	0.52	19479.22	248.14
56	1.03	25	1	50	100	93.4	0.41	20215.12	257.52	120.2	0.77	35130.02	447.52	111.7	0.41	21153.66	269.47
57	1.045	11	2	70	150	81.9	0.62	90639.81	1154.65	99.0	0.78	111741.93	1423.46	53.9	0.81	116393.25	1482.72
58	1.0642	11	1	70	150	69.9	0.66	98058.13	1249.15	97.3	0.88	119794.92	1526.05	102.9	0.70	101467.89	1292.58
59	1.045	11	2	30	100	25.6	0.66	40398.85	514.64	48.4	0.81	47920.44	610.45	55.5	0.89	52172.50	664.62
60	1.045	25	2	30	400	240.50	0.61	24245.45	308.86	283.8	0.78	28098.06	357.94	236.0	0.42	17690.23	225.35
61	1.045	17	1	50	100	178.20	0.72	51216.30	652.44	67.6	0.27	22680.32	288.92	60.6	0.53	44896.44	571.93
62	1.0642	25	2	50	100	141.80	0.65	15829.23	201.65	125.0	0.77	18782.64	239.27	105.3	0.48	13697.57	174.49
63	1.03	25	1	30	250	208.30	0.19	7162.98	91.25	270.6	0.56	24906.64	317.28	126.6	0.49	29191.57	371.87
64	1.03	11	2	70	250	264.20	0.77	158588.11	2020.23	234.0	0.42	100466.62	1279.83	185.8	0.75	159674.60	2034.07
65	1.03	11	2	30	150	69.9	0.86	74983.96	955.21	64.1	0.80	70190.39	894.15	68.3	0.80	69836.25	889.63
66	1.045	17	1.5	30	100	44.3	0.62	27545.08	350.89	47.0	0.68	30435.58	387.71	45.9	0.55	24757.67	315.38
67	1.03	25	2	70	150	163.50	0.41	31497.52	401.24	198.6	0.65	40784.44	519.55	233.3	0.56	40827.30	520.09
68	1.03	11	2	70	250	161.50	0.75	168485.09	2146.31	223.7	0.59	138238.07	1760.99	210.5	0.61	138476.57	1764.03
69	1.045	25	1	70	150	196.30	0.57	49279.48	627.76	118.2	0.49	47382.42	603.60	100.5	0.37	36286.62	462.25
70	1.03	11	1.5	30	150	81.8	0.77	79218.03	1009.15	55.5	0.77	85431.49	1088.30	61.2	0.83	88940.47	1133.00
71	1.0642	17	2	50	150	149.50	0.55	37200.53	473.89	152.5	0.53	36298.00	462.39	159.4	0.61	40682.17	518.24
72	1.0642	11	2	30	100	55.8	0.85	46780.80	595.93	47.3	0.70	40212.18	512.26	77.5	0.73	40652.83	517.87
73	1.03	17	1	30	400	248.30	0.64	73407.31	935.12	244.3	0.23	23512.99	299.53	221.1	0.67	87364.57	1112.92
74	1.0642	17	1	50	400	323.80	0.50	57943.41	738.13	385.4	0.67	73781.32	939.89	338.1	0.67	76029.30	968.53
75	1.0642	17	1	50	150	114.70	0.61	54356.73	692.44	139.5	0.61	52629.70	670.44	154.6	0.58	47627.00	606.71
76	1.0642	11	2	70	400	315.80	0.75	209831.64	2673.01	281.5	0.73	216069.51	2752.48	174.6	0.70	236066.31	3007.21

DEISGN POINTS					Rep I				Rep II					Rep III			
	W	S	BQ	AP	P	A	B	C	D	A	B	C	D	A	B	C	D
77	1.0642	11	1.5	30	150	91.3	0.75	71536.45	911.29	93.1	0.85	81522.24	1038.50	98.7	0.43	37257.70	474.62
78	1.03	25	1.5	30	150	95.1	0.41	12335.77	157.14	104.5	0.36	11194.51	142.61	96.9	0.31	9618.42	122.53
79	1.045	11	1.5	50	100	42.1	0.71	68470.32	872.23	86.7	0.89	81018.32	1032.08	55.1	0.71	67373.00	858.25
80	1.0642	17	2	50	400	414.4	0.64	62737.98	799.21	329.5	0.18	21192.05	269.96	1073.7	0.25	25959.59	330.70
81	1.0642	25	1	30	250	273.7	0.56	16669.21	212.35	217.8	0.45	12592.20	160.41	188.3	0.34	9689.68	123.44
82	1.0642	11	1.5	70	250	191.9	0.66	137823.15	1755.71	244.3	0.77	158545.33	2019.69	144.8	0.64	139633.12	1778.77
83	1.0642	11	1.5	50	250	148.3	0.66	127970.62	1630.20	208.0	0.35	75745.16	964.91	284.6	0.85	122620.12	1562.04
84	1.03	25	2	70	250	513.1	0.48	42710.29	544.08	379.6	0.61	49554.50	631.27	241.4	0.41	42234.22	538.02
85	1.03	17	2	30	250	175.9	0.54	35318.90	449.92	107.6	0.50	34446.51	438.81	147.6	0.64	43357.82	552.33
86	1.03	17	1.5	30	400	204.5	0.52	61051.66	777.73	264.5	0.47	48359.96	616.05	345.9	0.52	52307.52	666.34
87	1.03	25	1	70	100	162.5	0.76	35276.91	449.39	88.1	0.36	27280.13	347.52	519.5	0.75	28430.30	362.17
88	1.0642	25	1.5	70	400	530.5	0.52	42725.00	544.27	434.1	0.69	40756.88	519.20	552.8	0.56	42035.79	535.49
89	1.03	17	1.5	50	250	408.1	0.75	74418.49	948.01	155.9	0.52	75440.69	961.03	163.5	0.64	92636.86	1180.09
90	1.03	17	2	50	100	83.9	0.27	16131.46	205.50	98.5	0.61	36050.38	459.24	98.7	0.71	41655.98	530.65
91	1.045	25	1.5	70	400	516.0	0.71	58731.19	748.17	1295.2	0.49	47154.63	600.70	447.6	0.78	63481.32	808.68
92	1.045	17	1.5	70	400	279.1	0.65	158205.36	2015.35	298.6	0.53	123105.07	1568.22	283.8	0.55	139079.09	1771.71
93	1.0642	17	2	50	100	95.3	0.81	37833.57	481.96	115.2	0.61	32203.20	410.23	84.7	0.28	14766.40	188.11
94	1.045	17	2	70	250	225.2	0.53	85128.47	1084.44	250.0	0.59	90583.44	1153.93	192.1	0.84	117921.66	1502.19
95	1.0642	17	1.5	70	250	411.2	0.67	60513.55	770.87	266.1	0.17	33664.26	428.84	277.5	0.67	81068.74	1032.72
96	1.045	11	1	50	400	248.0	0.09	32413.74	412.91	296.5	0.83	202035.36	2573.70	281.6	0.75	187857.72	2393.09
97	1.03	17	1.5	30	400	184.5	0.61	67083.81	854.57	206.7	0.54	60103.18	765.65	474.2	0.71	65141.62	829.83
98	1.03	25	1	50	150	147.7	0.56	30017.19	382.38	155.0	0.65	40458.68	515.40	149.7	0.56	31468.06	400.87
99	1.03	17	1.5	70	100	99.8	0.82	63452.10	808.31	81.1	0.61	52584.84	669.87	76.1	0.61	53628.95	683.17
100	1.03	25	1.5	50	400	346.6	0.61	50683.75	645.65	329.1	0.38	31004.20	394.96	493.6	0.75	44298.83	564.32
101	1.0642	25	1	50	250	235.3	0.39	19277.93	245.58	421.6	0.74	29164.57	371.52	556.1	0.45	19496.30	248.36
102	1.03	25	2	50	400	349.8	0.48	35620.73	453.77	319.7	0.38	29287.23	373.09	314.2	0.03	1706.14	21.73
103	1.0642	17	1	70	400	530.0	0.81	77150.60	982.81	377.2	0.55	90147.63	1148.38	1021.1	0.81	64593.30	822.84
104	1.0642	11	1	50	400	202.2	0.77	181224.68	2308.59	521.8	0.64	122710.70	1563.19	215.5	0.70	173849.10	2214.64
105	1.03	17	1	70	150	139.6	0.75	85974.49	1095.22	155.3	0.64	80378.73	1023.93	103.1	0.50	67079.41	854.51
106	1.03	11	1.5	30	100	51.2	0.85	64179.18	817.57	31.0	0.68	53394.92	680.19	116.1	0.70	53149.27	677.06

DEISGN POINTS					Rep I					Rep II					Rep III						
	W	S	B	Q	A	P	A	B	C	D	A	B	C	D	A	B	C	D			
107	1.045	11	2	50	100	67.8	0.52	456	94.59	582.10	77.4	0.81	714	44.97	910.13	44.7	0.71	634	54.32	808.34	
108	1.064	21	7	1.5	70	100	75.4	0.46	383	65.77	488.74	145.7	0.61	476	94.6	607.57	115.7	0.31	263	06.08	335.11

Appendix E. Blue Dart

Why is it important to model atmospheric variations in High Energy Laser (HEL) propagation modeling?

High Energy Lasers (HEL) weapons are intriguing weapons. They travel at the speed of light, engage targets with bullet-like precision from extremely long ranges, make little noise without being seen, and typically leave little to no collateral damage behind. So are lasers the solution for which we have been looking? Well, aside from the many advantages listed, they are not “all weather” weapons. This likely means lasers will always be used in combination with other weapons, as they may be useless on rainy or poor visibility days. However, there are still ways in which we can try to maintain laser performance on such days.

Atmospheric effects can absorb, scatter, and bend light, causing a laser beam to diminish as it propagates. These effects are constantly changing as a function of a dynamic atmosphere with temperature and density differentials. We cannot control the atmosphere, however, we can attempt to develop durable HEL weapon designs which can withstand a variety of weather conditions, and identify altitudes and geometries which have the least negative impact on laser propagation. So how do we figure out which designs and geometries are best? Live tests can yield insights to best system designs and engagement geometries; however, since HEL tests are infrequent, data is very limited. Modeling and simulation of HEL weapons is an efficient and cost effective alternative to live tests. Directed Energy Joint forces (Air Force, Army, Navy) are extensive users of HEL models for HEL research and development (R&D). These models are highly capable and helpful when assessing conceptual HEL designs or enhancing predictive modeling capabilities for existing HEL weapons.

One limitation of HEL models addressed in this research is the deterministic nature of models used. This means the atmosphere is modeled, however only a snap shot of the atmosphere in time, with no variation through time. An independent repeat of one simulation will yield identical results to the first, which is unlike a repeat of a live test, which will yield different results as a function of the changing atmosphere. When trying to represent a realistic environment for HEL propagation, stochastic models are most

appropriate. Stochastic models of the atmosphere capture the entire spectrum of weather conditions seen in a location over a period of time. These conditions are pulled at random, to simulate a randomly varying atmosphere.

The primary objective for modeling a stochastic atmosphere in this research was to determine HEL designs and engagement geometries best suited for varying weather conditions. In other words, identify which laser characteristics are most influenced by weather. A realistic atmosphere was modeled through obtaining real weather data from meteorological reports (METARs), and incorporating those points into the HEL modeling process. METARs are daily reports for aviators needing to know ground conditions (temperature, dew point, visibility, etc.) in multiple geographic locations around the globe. These observations capture variations found naturally in the atmosphere, and in turn, allow us to estimate how an HEL system would perform in both good and bad weather conditions. An experimental test design was used to lay out the sequence of simulations ran. This experimental design is based on Design of Experiment (DOE) methodology, which varies multiple factors during the simulation, in order to see the effect of interactions that exist between laser, platform, geometry, and atmospheric parameters.

For this research, an Airborne B1-B was modeled, equipped with an HEL weapon which was engaging a target on the ground. Results found that different HEL weapon designs modeled each do perform differently given different weather conditions. And actually, some HEL designs diminished right away as a result of the poor visibility within the atmosphere. Non-linear interactions were identified from the HEL model, showing non-linear relationships between laser characteristics and intensity on target, as well as non-linear relationships between laser characteristics and atmospheric effects. The way in which the atmospheric data was incorporated into the model, and the experimental design, allows us to differentiate between a performance outcome due to interferences, parameter settings, or a combination of both. This was a very effective model for predicting laser weapon performance.

Modeling HEL weapons is not only effective in identifying relationships between parameters in a complex and highly non-linear space, but it can also be effective in

designing live tests. Estimates of the best test designs can be determined prior to tests, through modeling and simulation. Using METAR data from the location of test can easily be incorporated, to give a user a representative model of the range of atmospheric conditions in their geographic location.

Bibliography

1. Anderberg B. and Wolbarsht M. L. *Laser Weapons*. New York: Plenum Press, 1992.
2. Andrews L. C and Phillips R. L. *Laser Beam Propagation through Random Media*. (2nd Edition). Bellingham, WA: SPIE Optical Engineering Press, 2005.
3. Bagnell, Richard. HEL Modeling Subject Matter Expert. Personal Correspondence. July 2011.
4. Fiorino, Steven. Atmospheric & HEL Modeling Subject Matter Expert. Personal Correspondence. July 2011.
5. Fiorino S.T., Bagnell R.J., Krizo M. J. and Cusumano S.J. *Propagation Variability Assessments of Ship Defense HEL and HPM Performance in Worldwide Maritime Boundary Layer Environments at Wavelengths of 1.0642 μm , 2.141 μm , 3.16 μm , and 12.2 cm*. Wright Patterson AFB, OH: Air Force Institute of Technology, 2008.
6. Committees, United States Government Accountability Office Report to Congressional. "Defense Aquisitions: Assessment of Selected Major Weapons Programs." March 2005.
7. Long S. N. *Characterizng Effects and Benefits of Beam Defocus on High Energy Laser Performance Under Thermal Blooming and Turbulence Conditions for Air-to-Ground Engagements*. PhD Dissertation. Dayton, OH: Air Force Institute of Technology, 2008.
8. Montgomery D. C. *Design of Experiments* (7th Edition). New York, NY: John Wiley & Sons, Inc., 2009.
9. Perram G. P., Cusumano S. J., Hengehold R. L., and Fiorino S. T. *An Introduction to Laser Weapon Systems*. Albuquerque, N.M.: The Directed Energy Professional Society, 2010.
10. Ponack R. S. and Miller J. O. "Capability Assessment of the High Energy Laser Liquid Area Defense System (HELLADS)." *Journal of Directed Energy Vol 3*. (Directed Energy Professional Society), Winter 2010: 193-211.

11. Richardson L. F. *Weather Prediction by Numerical Process*. Cambridge, U.K.: Cambridge University Press, 1922.
12. Rockower E.B. *Laser Propagation Code Study*. Monterey, CA: DTIC, 1985.
13. Souder J. K. and Langille D. B. "How Directed Energy Benefits the Army". *Army Science Conference (24th) proceedings*. Huntsville, AL: 2005
14. Wisdom B. W. *Assessment of Optical Turbulence Profiles Derived from Probabalistic Climatology*. Masters Thesis. Dayton, OH: Air Force Institute of Technology, 2007.
15. 14th Weather Squadron METAR. July 2011.
<https://notus2.afccc.af.mil/SCIS/services/mission.asp>

REPORT DOCUMENTATION PAGE				Form Approved OMB No. 074-0188	
<p>The public reporting burden for this collection of information is estimated to average 1 hour per response, including the time for reviewing instructions, searching existing data sources, gathering and maintaining the data needed, and completing and reviewing the collection of information. Send comments regarding this burden estimate or any other aspect of the collection of information, including suggestions for reducing this burden to Department of Defense, Washington Headquarters Services, Directorate for Information Operations and Reports (0704-0188), 1215 Jefferson Davis Highway, Suite 1204, Arlington, VA 22202-4302. Respondents should be aware that notwithstanding any other provision of law, no person shall be subject to a penalty for failing to comply with a collection of information if it does not display a currently valid OMB control number.</p> <p>PLEASE DO NOT RETURN YOUR FORM TO THE ABOVE ADDRESS.</p>					
1. REPORT DATE (DD-MM-YYYY) 9-15-2010		2. REPORT TYPE Thesis		3. DATES COVERED (From - To) Sept 2010 - Sept 2011	
4. TITLE AND SUBTITLE MODELING AND ANALYSIS OF HIGH ENERGY LASER WEAPON SYSTEM PERFORMANCE IN VARYING ATMOSPHERIC CONDITIONS				5a. CONTRACT NUMBER	
				5b. GRANT NUMBER	
				5c. PROGRAM ELEMENT NUMBER	
6. AUTHOR(S) Melin, Megan, P., Civilian DR-II, USAF				5d. PROJECT NUMBER	
				5e. TASK NUMBER	
				5f. WORK UNIT NUMBER	
7. PERFORMING ORGANIZATION NAMES(S) AND ADDRESS(S) Air Force Institute of Technology Graduate School of Engineering and Management (AFIT/EN) 2950 Hobson Street, Building 642 WPAFB OH 45433-7765				8. PERFORMING ORGANIZATION REPORT NUMBER AFIT-OR-MS-ENS-11-27	
9. SPONSORING/MONITORING AGENCY NAME(S) AND ADDRESS(ES) AFRL/RD/RDTAE Attn: Mr. Kevin Sparks 3550 Aberdeen Ave SE KAFB NM 87111 DSN: 246-7700 e-mail: Kevin.sparks@kirtland.af.mil				10. SPONSOR/MONITOR'S ACRONYM(S)	
				11. SPONSOR/MONITOR'S REPORT NUMBER(S)	
12. DISTRIBUTION/AVAILABILITY STATEMENT APPROVED FOR PUBLIC RELEASE; DISTRIBUTION UNLIMITED.					
13. SUPPLEMENTARY NOTES					
14. ABSTRACT This thesis addresses two primary concerns relating to Directed Energy (DE) models and tests: need for more use of Design of Experiment (DOE) in structuring DE models and tests, and lack of modeling atmospheric variability in High Energy Laser (HEL) weapon system propagation models and tests. To address these concerns we use a DOE factorial design to capture main, interaction, and non-linear effects between modeled weapon design and environmental factors in a well defined simulated Air-to-Ground HEL engagement scenario. The scenario modeled considers a B1-B aircraft in the 2022 timeframe equipped with an HEL weapon, irradiating a ground target from 30K feet altitude. The High Energy Laser End-to-End Operational Simulation (HELEEOS), developed by the AFIT Center for Directed Energy (CDE), is used to model HEL propagation. Atmospheric variability is incorporated by using input from the Laser Environmental Effects Definition and Reference (LEEDER) model based on randomly selected daily meteorological data (METAR) for a specific geographic location. Results clearly indicate the practical significance of a number of HEL weapon design and environmental factors, to include a number of previously unidentified interactions and non-linear effects, on the final energy delivered to a target for our modeled scenario.					
15. SUBJECT TERMS Directed Energy, High Energy Laser Modeling, Design of Experiment, Response Surface Methodology, HELEEOS, LEEDR					
16. SECURITY CLASSIFICATION OF:			17. LIMITATION OF ABSTRACT	18. NUMBER OF PAGES 98	19a. NAME OF RESPONSIBLE PERSON John O. Miller, PhD (ENS)
a. REPORT U	b. ABSTRACT U	c. THIS PAGE U			19b. TELEPHONE NUMBER (Include area code) (937) 255-6565, ext 4326; e-mail: John.Miller@afit.edu

Standard Form 298 (Rev. 8-98)
Prescribed by ANSI Std. Z39-18